Quaternary International 417 (2016) 16–38

Contents lists available at ScienceDirect

Quaternary International

journal homepage: www.elsevier.com/locate/quaint

Formation processes and stratigraphic integrity of the Middle-to-Upper Palaeolithic sequence at Cova Gran de Santa Linya (Southeastern Prepyrenees of Lleida, Iberian Peninsula)

Ana Polo-Díaz [a, *], Alfonso Benito-Calvo [b], Jorge Martínez-Moreno [c], Rafael Mora Torcal [c]

[a] Department of Geography, Prehistory and Archaeology, Francisco Tomás y Valiente S/N, 01006 Vitoria-Gasteiz, University of the Basque Country (UPV-EHU), Spain
[b] Centro Nacional de Investigación sobre Evolución Humana (CENIEH), Paseo Sierra de Atapuerca 3, 09002 Burgos, Spain
[c] Centre d'Estudis del Patrimoni Arqueològic de la Prehistoria, Facultat de Lletres, Universitat Autònoma de Barcelona, 08193 Bellaterra, Spain

ARTICLE INFO

Article history:
Available online 30 November 2015

Keywords:
Middle-to-Upper Palaeolithic transition
Geoarchaeology
Formation processes
Microstratigraphy
Cova Gran
Iberian Peninsula

ABSTRACT

Sediments from Cova Gran de Santa Linya (Southeastern Prepyrenees of Lleida, Iberia) are investigated by geoarchaeological means.

Micromorphological, textural, quartz grain morphoscopy and geochemical analyses are coupled with stratigraphic and sedimentary macroscopic data to provide new insights into the formation processes and the integrity of the occupation layers and embedded sterile deposit documented at the Middle-to-Upper Palaeolithic boundary.

Direct indicators of the anthropogenic and natural dynamics involved in the deposition and alteration of the sediments investigated are provided.

Results reveal the presence of *in situ* combustion structures as a major sedimentary indicator of human activity and occupation surfaces at the site. The overall good preservation of the combustion residues indicates that occupation layers have been preserved in their original context of deposition. Traits of surface exposure in parallel to progressive lessening of evidence related to human activity at the top of the Middle Palaeolithic sequence suggest discontinuity in the occupation of the site and a possible abandonment of the rock-shelter at the end of this period.

Formation processes of the sterile deposit documented between the Mousterian and the Early Upper Palaeolithic levels involved the accumulation of debris from local sediments and soils as well as from the structure of the rock-shelter.

Soil-forming dynamics related to palaeoenvironmental moisture fluctuations have also been recorded throughout the sequence investigated and indicate periods of surface stability during the formation of the sterile deposit.

Environmental dynamics active during the formation of the sterile partially disturbed the top of the Mousterian layer, however, our data indicate that such dynamics did not substantially affect the overall integrity of the archaeological record.

Our results highlight the crucial contribution of geoarchaeology and microstratigraphy to the characterisation and assessment of the anthropogenic and natural dynamics involved in the accumulation and taphonomy of Middle-to-Upper Palaeolithic sequences.

1. Introduction

Sediments from archaeological sites, through the investigation of their formation processes, have the potential to provide direct indicators on human behaviour and palaeoenvironmental contexts of prehistoric groups. They can also contribute key data concerning

* Corresponding author.
E-mail address: anapolodiaz@gmail.com (A. Polo-Díaz).

http://dx.doi.org/10.1016/j.quaint.2015.10.113
1040-6182/

the preservation state and taphonomy of occupation layers and deposits as a whole.

Understanding the formation processes of sediments is especially relevant to the investigation of the Middle-to-Upper Palaeolithic (MUP) transition in the Iberian Peninsula. The integrity of some of the sequences studied in the region has been questioned (Zilhão and d'Errico, 1999; Zilhão, 2006a, 2006b) and has been the subject of debate (Bernaldo de Quirós et al., 2008; Soler i Subils et al., 2008), fuelling discussion regarding settlement strategies and cultural continuity or discontinuity of human populations and related Middle and Upper Palaeolithic industrial complexes.

In parallel the potential role of palaeoclimate as a triggering factor of ecological constrains that might have favoured the MUP change in the region has gained increasing interest and has contributed relevant insights into the discussion (d'Errico and Sanchez Goñi, 2003; Finlayson and Carrión, 2007; Sepulchre et al., 2007; Schmidt et al., 2012; Banks et al., 2013).

However, little direct data is actually available from MUP contexts regarding the stratigraphic patterns, composition, palaeoenvironments and the syn/post-depositional history of artefact bearing sediments.

Geoarchaeology provides tools to investigate the formation processes of archaeological deposits through the analysis of cultural, palaeoenvironmental and taphonomic sedimentary contexts (Goldberg and Macphail, 2006; Goldberg and Sherwood, 2006; Goldberg and Berna, 2010; Karkanas and Goldberg, 2013), which in turn allows the assessment of the integrity of stratigraphic records.

The application of geoarchaeological techniques and particularly micromorphology to the study of Middle Palaeolithic (MP) contexts in the Iberian Peninsula has provided high-resolution data for the understanding of key human behaviour as the management of fire and the spatial distribution of activity areas within the sites (Gómez de la Rúa et al., 2010; Vallverdú et al., 2010; Courty et al., 2012).

In addition, stratigraphic and sedimentary analyses have contributed relevant information to the identification of palaeoenvironmental dynamics in the origin of erosive contacts at the base of some Upper Palaeolithic (UP) sequences (Aubry et al., 2011).

Insights into the role of palaeoclimatic trends involved in the accumulation and preservation of archaeological records at the MUP boundary have also been contributed through the application of microscopic techniques (Courty and Vallverdù, 2001; Angelucci and Zilhaõ, 2009; Angelucci et al., 2013; Galván et al., 2014; Kehl et al., 2014).

In this context the application of micromorphology as an essential tool for the assessment of the integrity and preservation degree of MP sequences in the region has been highlighted (Mallol et al., 2010).

However, and despite the advances achieved in this field, systematic implementation of geoarchaeological analyses focused on the formation processes of sediments from Iberian MUP transitional sequences is still needed (Mallol et al., 2012) in order to improve our understanding of the interactions between humans and environments in such contexts and the implications of such relationships for the definition of cultural models.

This paper presents the results of the investigations on the formation processes and stratigraphic integrity of the sediments from the MUP sequence of Cova Gran de Santa Linya (Southeastern Prepyrenees of Lleida, Iberia). This rock-shelter holds a wide archaeological record with clearly defined Middle and Early Upper Palaeolithic occupation levels interspersed by sterile deposits. One of these steriles in particular is characterised by a discontinuity in the accumulation of artefacts of about 20–50 cm thick between the Late MP and the Early UP levels (Martínez-Moreno et al., 2010; Mora et al., 2011, under review). This discontinuity however, seems to loose definition in the westernmost area of the MUP transitional sequence, where Mousterian artefacts cut across different sedimentary units.

This work aims to clarify the depositional and post-depositional dynamics involved in the formation processes of sediments from the Late MP and the Early UP occupations at the site as well as from the sterile deposit documented between them. At the same time the dynamics behind the apparent local vertical dispersion of Mousterian artefacts are investigated together with the overall integrity of the archaeological record at the MUP boundary. The following research objectives are addressed:

- To characterise traits of human activity in the sediments associated with artefact accumulations from the Late MP and the Early UP levels;
- To determine the composition and formation history of the sterile between the Late MP and the Early UP levels;
- To provide sedimentary and stratigraphic parameters for the assessment of the preservation degree, taphonomy and integrity of the MUP sequence;

2. The site of Cova Gran

Cova Gran is a south-facing rock-shelter (0°48′45.78″E, 41°55′37.65″N, WGS84), forming a semi-vaulted roof, 92 m wide, 83 m deep and 25 m high. It is situated in the south margin of the Marginal Sierras of the Eastern Pyrenees (Lleida, Spain), close to their link with the Tertiary Ebro Depression (Fig. 1).

2.1. Geological and geomorphological background and current climatic conditions

The geological setting of the rock-shelter is characterised by Jurassic and Cretaceous formations overlying a Triassic evaporite substratum (Fig. 1B). Cova Gran is located at 385 m a.s.l. at the bottom of the Sant Miquel ravine, a tributary of the Noguera-Pallaresa river on the western side of the Segre main watercourse. The Sant Miquel ravine forms a small V-shaped valley, incised more than 250 m, that developed following the area of weakness defined by mechanical contact between the Late Cretaceous Bona Formation and the clays and gypsums of the Upper Triassic (Fig. 1B). This E–W contact is displaced by transversal faults, which cause minor variation in the valley direction, forming incised meanders. Cova Gran is situated in the concave side of one of these incised meanders, coinciding with a limestone area that was weakened by faulting (Benito-Calvo et al., 2009). The rock-shelter developed in the above-mentioned Bona Formation, which consists of bioclastic limestones, calcarenites, sandstones and bioconstructions, materials that formed in a shallow marine environment (Simó, 2004). The limestones in Cova Gran include fault breccias, composed by subangular and subrounded limestone clasts and cemented by a fine-grained reddish matrix.

The current climatic conditions in the area of the site are temperate with dry or hot summer, an average annual temperature of 13–14 °C, a temperature range between 19 and 20 °C and an

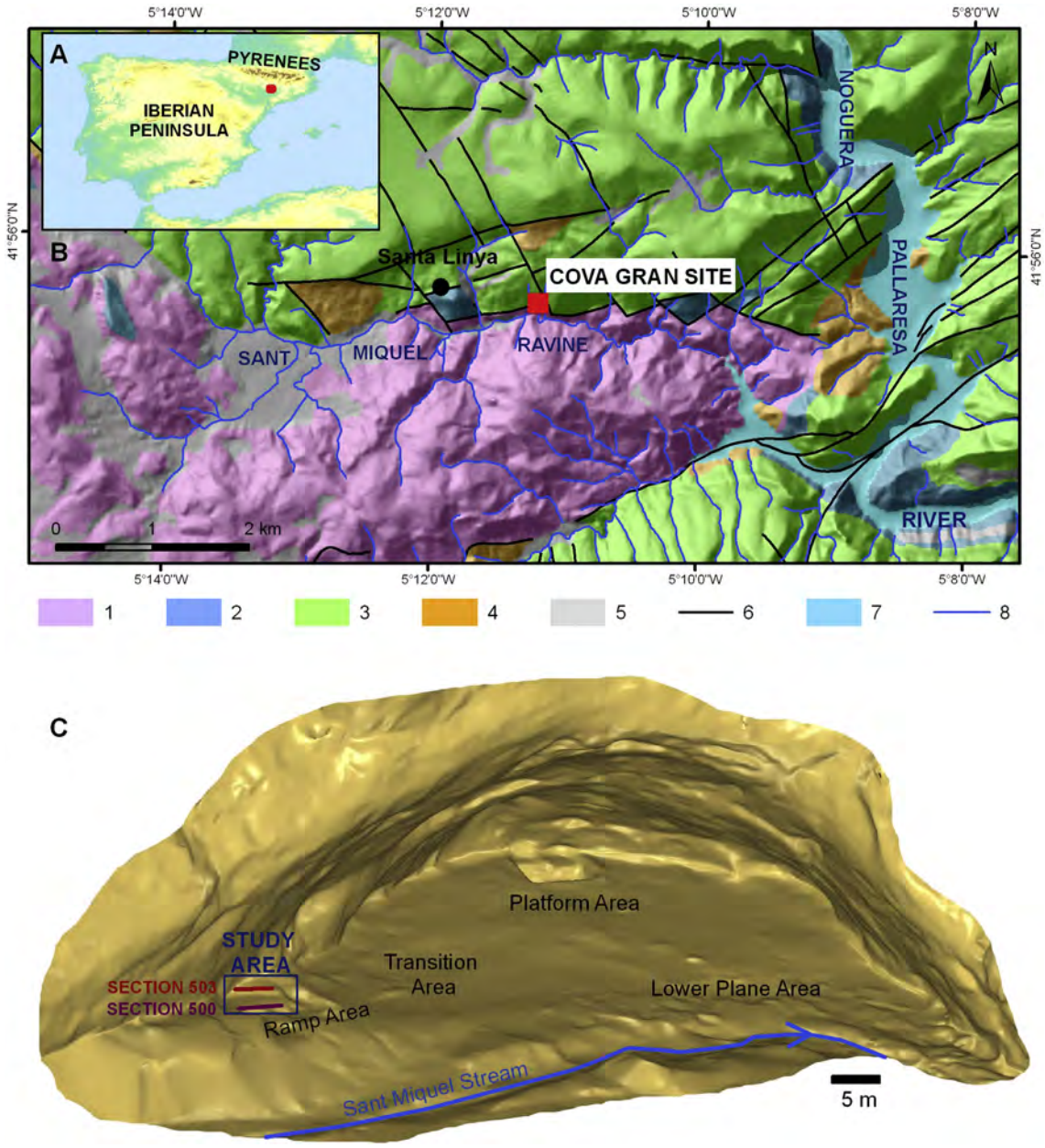

Fig. 1. Cova Gran geological and geomorphological map. A) General location of the site in the Iberian Peninsula. B) Geological map of the region. Legend: 1, Triassic; 2, Jurassic; 3, Cretaceous; 4, Tertiary; 5, Quaternary, 6; Faults; 7, Reservoir; 8, Drainage network. C) Shaded 3D model of the Cova Gran site carried out by lasser scanning (Leica C10). Note the Ramp sector and the study area at the western part of the rock-shelter.

average annual precipitation between 500 and 550 mm (Ninyerola et al., 2005; Servei Meteorològic de Catalunya, 2014). Such values situate Cova Gran in a transitional climatic area between the Pyrenees and the Ebro Basin where more extreme environmental conditions prevail.

2.2. Stratigraphy and archaeological sequence

The sedimentary record of Cova Gran began to be explored in 2004 and given the depth and extension of the deposit the full extent of the archaeological stratigraphy remains unknown. Within the rock-shelter a sedimentary infill reaching 3–9 m above the ravine bed with four clearly differentiated morphological areas has been delimited (Fig. 1C). Test-pitting and open-area excavations undertaken in each of the individualised sectors have uncovered a broad chrono-cultural sequence including MP, Early UP and Late Prehistory levels (Mora et al., 2011, 2014).

The sediments investigated in this work are from the MUP sequence documented at the site, which is located in the western part of the rock-shelter, on a lateral ramp with a total area of 200 m^2 and a mean slope of 14° towards the East (Ramp sector). Approximately 40 m^2 of the Ramp total area have been excavated to date unearthing seven consecutive archaeological levels, four of them attributed to the MP and three to the Early UP (Fig. 2C). In this sector, sediments consist basically of unconsolidated clast-supported breccias, which were divided in two general lithostratigraphic units referred to as 497 and S1 in reference to the differences observed at the top and bottom respectively of the stratigraphy.

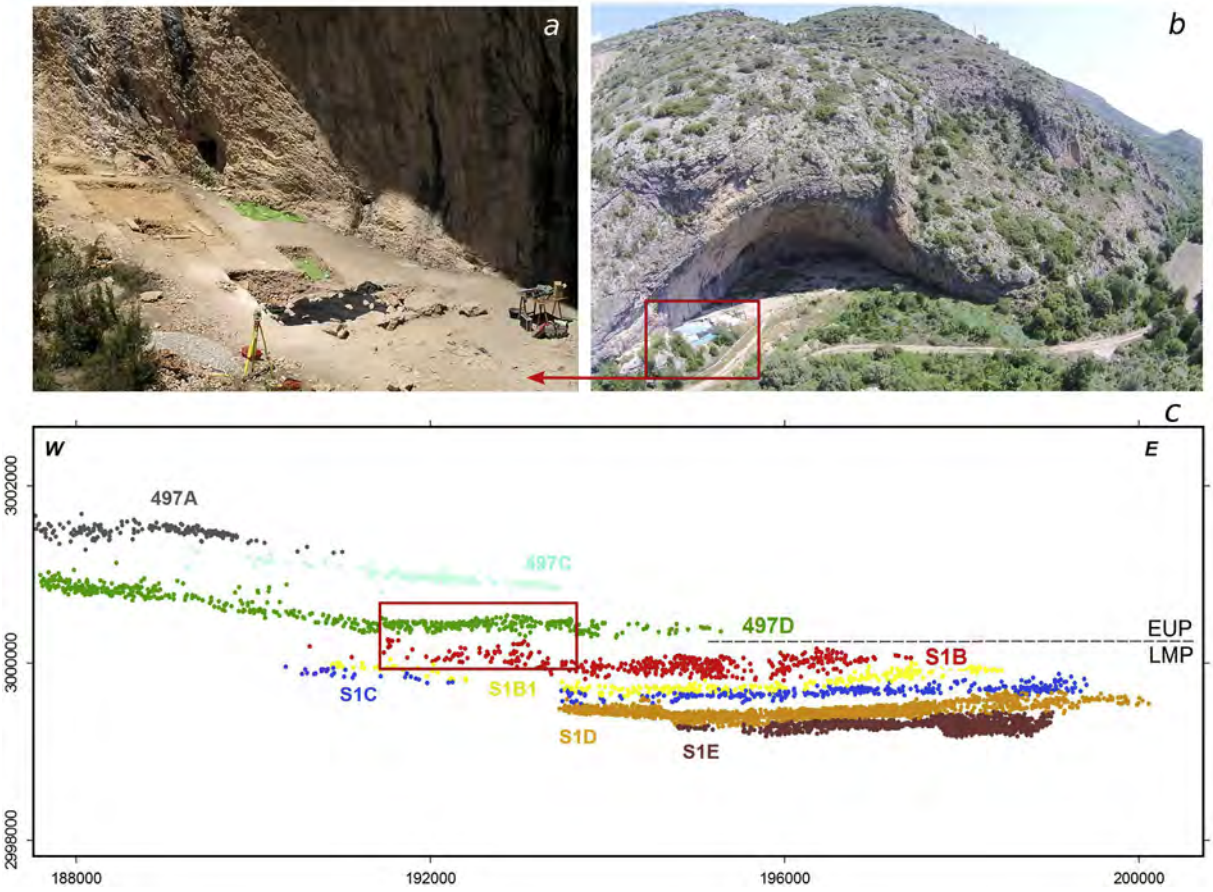

Fig. 2. a) Ramp sector where the MUP transitional sequence has been documented. b) General view of Cova Gran rock-shelter. The red box marks the location of the Ramp sector. Views in a) and b) are from the South. c) Archaeostratigraphic levels and artefact distribution of MP and Early UP levels in the Ramp sector showing the entire excavation trench. The red box marks the area investigated in this work (see detail in Fig. 3). Grid values in millimeters. (For interpretation of the references to colour in this figure legend, the reader is referred to the web version of this article.).

Unit 497, is defined by subrounded and subangular clasts containing abundant fine-grained matrix, massive or poorly bedded, which dips 12° towards the East. The sand and clay matrix contains calcite, quartz, and smaller amounts of illite, albite and clinochlore (Benito-Calvo et al., 2009). Sedimentary Unit 497 holds the later UP archaeological levels 497A and 497C.

S1 lithostratigraphic unit is composed basically of subangular breccias with general scarce fine-grained matrix content and strata dipping towards the East in the western area and towards the West in the eastern area of the Ramp sector. Matrix in S1 unit is mainly composed of calcite and dolomite, some quartz and illite, and to a lesser extent, of clinochore and gypsum (Benito-Calvo et al., 2009).

Sedimentary Unit S1 encloses the MUP change and presents internal stratification comprising from bottom to top five sedimentary sub-units or facies: S1-30, S1-25, S1-20, S1-10 and S1-05 (Fig. 3A).

It also holds two archaeological levels: S1B, attributed to the MP and 497D assigned to the Early UP. Details on the chronological frame of these two levels can be consulted elsewhere (Martínez-Moreno et al., 2010; Mora et al., 2011, under review).

Underlying S1B and S1-30 and also within S1 sedimentary unit, MP levels S1B1, S1C, S1D, S1E and S1F, currently under excavation, have been recorded in clast-supported beds of breccias (facies S1-40 and S1-50, Fig. 3A and 4A). These breccias are characterised by heterometric angular clasts and very scarce matrix. Among the clasts, these two beds occasionally show very local lenticular bodies of moderately sorted, fine-to-medium subangular pebbles.

Beds in the Ramp sector are gently dipping towards the east (Fig. 3A), which indicates a W or SW provenance for sediments coming mainly from outside. Nevertheless, towards the east of this area, MP layers dip westwards and display a gentle concave shape, as indicated by the geometry of the archaeological levels (Fig. 2C).

Here we refer to archaeological levels as concentrations of bone and lithic remains and related combustion residues documented during fieldwork.

3. Materials and methods

Micromorphological, textural, quartz grain morphoscopy and geochemical analyses were coupled with stratigraphic and sedimentary macroscopic data for the characterisation of sediments from the MUP transitional sequence in the western area of the Ramp sector. A section of approximately 70 cm in depth from exposed profiles (Fig. 3A and B) was sampled to cover the full vertical extension of the MUP sequence. In addition to block and bulk sediment samples, data from exposed surfaces of the excavation trench as well as from the immediate geological and sedimentary context of the site were recorded.

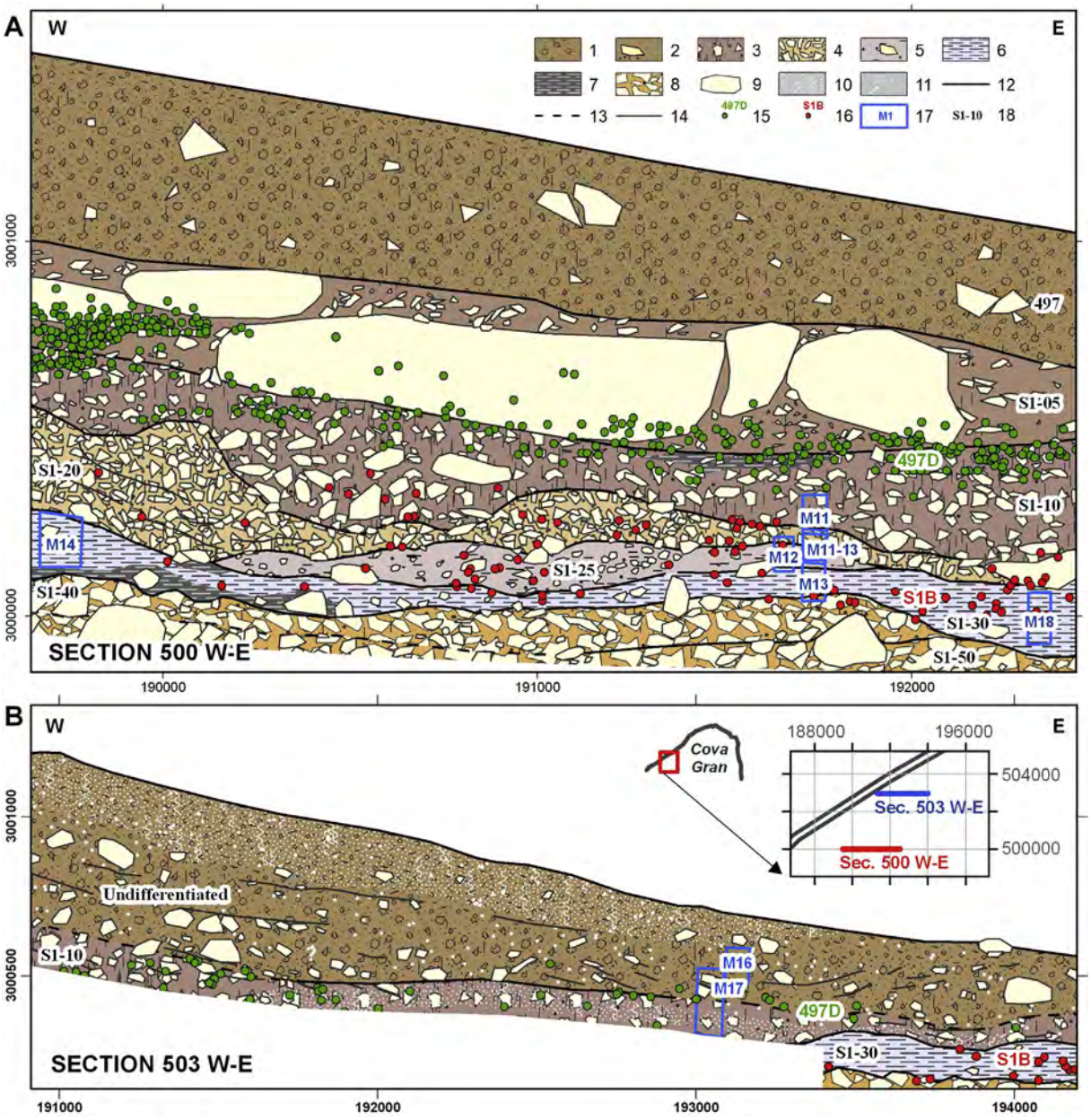

Fig. 3. Stratigraphic sections 500 EW (A) and 503 EW (B) of the Ramp sector studied in this work. Legend: 1, Massive and poorly bedded breccia containing abundant matrix and subrounded clasts; 2, Breakdown breccia; 3, Heterometric clast-supported breccia with reddish-brown loamy matrix; 4, Moderately sorted and poorly bedded breccia including scarce matrix and subrounded clasts; 5, Reworked ashes; 6, Ashy accumulation consisting of overlapping combustion structures; 7, Sediments rich in charred remains; 8, Clast-supported breccias with scarse matrix and heterometric angular clasts; 9, Limestone boulders and clasts; 10, Disperse powdery lime; 11, Carbonate nodules; 12, Stratigraphic boundaries; 13, Inferred stratigraphic boundary; 14, Bedding; 15, 497D archaeological artefacts; 16, S1B archaeological artefacts; 17, Block samples for micromorphological analysis; 18, Stratigraphic layers. Grid values in millimeters. (For interpretation of the references to colour in this figure legend, the reader is referred to the web version of this article.).

Consecutive oriented blocks of undisturbed sediments were collected for micromorphological analysis to provide data on the composition and the nature of the microstratigraphic contacts of facies S1-30, S1-25, S1-20 and S1-10.

Sediments overlaying S1-10, possibly related to facies S1-05, were also sampled.

Block samples were processed into eleven petrographic large thin sections (13.5 × 5.5 cm) at the micromorphology and image analysis laboratory of the University of Lleida (Spain). The slides were observed with a petrographic microscope at magnifications between 10X and 400X under Plane Polarized Light (PPL) and Crossed Polarized Light (XPL). International standard terminology was used for micromorphological description (Bullock et al., 1985; Courty et al., 1989; Stoops, 2003). Facies and microfacies criteria commonly applied in geology and accepted in archaeology were used for stratigraphic discrimination (Courty, 2001). Micromorphological individualisation of microfacies was based on similarities observed in composition and interrelation of features in terms of microfabric type. The slides were scanned on a flatbed scanner at high-resolution (1.200 dpi) in reflected light in order to allow observations at mesoscopic level (Arpin et al., 2002).

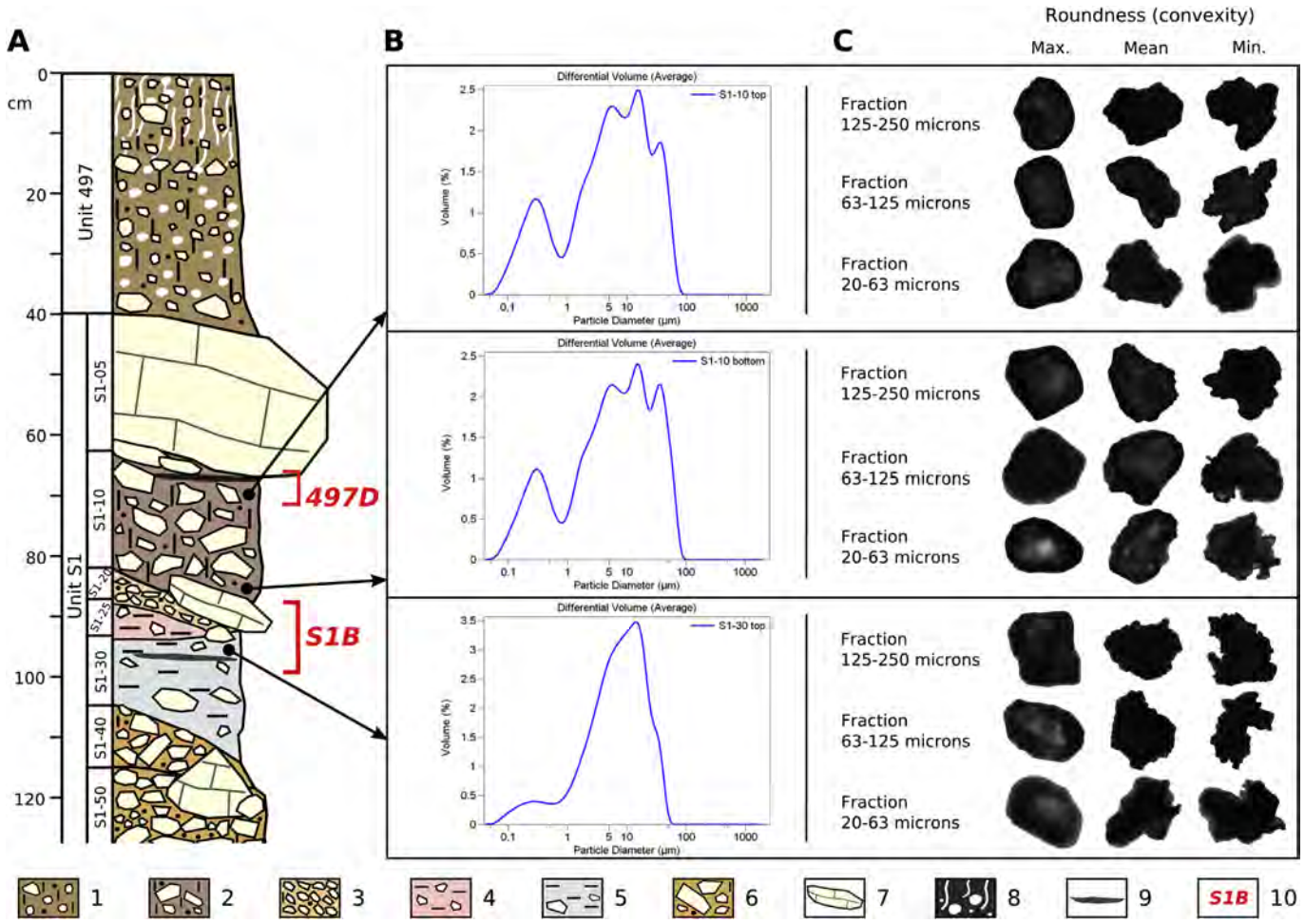

Fig. 4. A) Stratigraphic column representing the sequence in the Ramp sector along the section 500 EW (Fig. 3A). Note location of samples for grain size and particle roundness analyses. Legend: 1, Massive and poorly bedded breccia-conglomerate containing abundant matrix and subrounded clasts; 2, Heterometric clast-supported breccia with reddish-brown loamy matrix; 3, Moderately sorted and poorly bedded breccia including scarce matrix and subrounded clasts; 4, Reworked ashes; 5, Ashy accumulation; 6, Clast-supported breccias with scarce matrix and heterometric angular clasts; 7, Limestone boulders and clasts; 8, Pedogenic carbonates; 9, Sediments rich in charred remains; 10, Archaeological levels. B) Grain size distribution curves from Laser diffraction particle analysis of the fraction <63 μm. A Beckman Coulter LS 13 320 MW facility was used. Refractive index for the estimation: 1.64 real part and 0.1 imaginary part. Note similar grain size distribution patterns between curves from the top and bottom of facies S1-10. Both curves show polymodal grain size distribution with inputs of clayey silts and sands. This pattern is in agreement with inputs of sediments rich in soil materials observed in thin section. In contrast, distribution curve from the top of layer S1-B displays a pattern much more homogeneous as a result of a major input of medium/fine silts. This pattern is in agreement with the identification of ashes in this layer through micromorphology. C) Particle roundness analysis of the fractions 250–125, 125–63 and 63–20 μm estimated by the convexity parameter provided by microscopy Malvern Morphologi G3. Convexity is calculated by dividing the convex hull perimeter by the actual particle perimeter. Note particles displaying angular and subangular patterns both in facies S1-10 and S1-30, which suggests local source of sediments.

Samples for grain size, morphoscopy and WDXRF were collected from the top and bottom of facies S1-10 and S1-30 next to the block samples for micromorphological analysis (Fig. 4A).

Sieving and laser diffraction (Beckman Coulter LS 13 320 MW) were used for textural analysis and production of grain size distribution curves.

The Microscopy Malvern Morphologi G3 system was used to study the morphological parameters of the quartz grains of the fine-very fine sand and silt fractions from the sediments investigated to provide information regarding the sedimentary origin of the particles.

Bulk samples for Wavelength Dispersive X-Ray Fluorescence analysis (WDXRF) were processed using a PANalytical Axios spectrometer for compositional characterisation of major, minor and trace elements.

Detailed identification and mapping of the stratigraphy in Geographical Information System (GIS) were carried out using field surveying, ortophotos and 3D models obtained from 3D lasser scanning (Leica TPS 1200) and Photogrammetry (Photoscan Agisoft). These models were georeferenced in the site local coordinate system, created by means of a total station.

4. Results and discussion

4.1. The sedimentary evidence of the Late MP occupation: facies S1-30 and S1-25

4.1.1. Facies S1-30

Sediments from S1-30 are characterised by an approximately 25 cm thick whitish silty accumulation (Table 1). This facies rests on breccias associated mainly with gravity processes (facies S1-40, S1-50), including very local and limited water currents (Fig. 3A and 4A).

Table 1
Summary macroscopic and microscopic (micromorphological) characteristics of sediments investigated from the MUP transitional sequence of Cova Gran.

Facies S1	General characterisation	Thin section	Macroscopic data	Micromorphological features
S1-05	Roof collapse	CGM16 (lower section) CGM17 Top (?)	Clast-supported breccia, very poorly sorted, massive and heterometric. Angular platy limestone clasts. Abundant angular limestone boulders Reddish brown matrix (5 YR 6/4). Silty clay loam (35–50%). Small charcoal and bone fragments.	Mainly mineral accumulation. cf ratio 63 μm 60/40–70/30. Highly to moderately separated subangular-subrounded blocky microstructure. Peds show subhorizontal internal fissures and frequent bioreworking. Packing voids and bioturbation-related porosity. Calcitic crystallitic b-fabric. Coarse fraction random distribution. Heterometric rock fragments. Subangular limestone, calcitic crust and ophite fragments (≤5–6 cm). Quartz grains are predominantly angular and consist mainly of fine sands and silts. Angular medium-coarse quartz sand (≤2%). Coarse and fine subrounded −rounded silt (5% approx.). Very fine rounded sand (2% approx.). Abundant sediment aggregates rich in reddish clay and iron nodules. Frequent microcrystalline calcitic concretions with detrital inclusions. Carbonate dissolution and recrystallisation traits on rock fragments and calcitic features. Fresh (i.e.non-combusted) root and other plant tissue (≤2% − 500 μm approx.). Residual fresh and burnt bone fragments (≤150 μm). Pendants alternating micritic and sparitic layers are common and thicker than in S1-10. Fe–Mn staining and nodules, many of them in secondary position.
497D	Anthropogenic sediments + insitu combustion residues + Upper Palaeolithic artefacts	CGM17 Middle	Anthropogenic aggregates: Light brown (7.5 YR 6/4). Silty. 6–7 cm thick approx. Continuity along the profile. Combustion structures in the same sedimentary context.	Anthropogenic aggregates: Scattered reworked fragments of charred bone and plant tissue (≤300 μm). Yellowish subrounded aggregates (≤3000 μm) with sub-millimetric fragments of charcoal, charred bone and plant tissue embedded. Blackish subrounded sediment aggregates (≤3000 μm) with inclusions of partially burnt plant and bone tissue.
		497DCG7183	Combustion structure: Single combustion structure. Round-shaped. 60 cm diameter × 5 cm thickness approximately. Silty whitish-light brown (7.5 YR 7/4) layer at the top. Brownish grey (7.5 YR 4.1) layer at the bottom. Subcentrimetric and centrimetric rock fragments inclusions.	Ash layer: Homogeneous internal mineralisation of constituents. Calcitic residues from combustion of plant tissue including prismatic pseudomorphs in anatomical connexion (≤600 μm) and multicellular fragments (≤300 μm). Sediment aggregates (≤800 μm) with geogenic mineral inclusions. Strong bioturbation and calcitic recrystallisation. Charred layer: mixture of homogenously burnt rock-fragments, sediment aggregates and organic matter including bone fragments. Charred excrement patches (≤800/1000 μm) rich in plant remains and concentration of faecal spherulites. Strong bioturbation.
S1-10	Sterile Scattered Mousterian artefacts at the base	CGM17 Bottom	Clast-supported breccia, very poorly sorted, massive and heterometric. Angular platy limestone clasts (65–50%). Reddish brown matrix (5YR 6/4). Silty clay loam (35–50%). Comminuted charcoal and small fragments of bone. Lateral continuity and variable thickness. Sharp lower contact.	Mainly mineral accumulation. cf ratio 63 μm 60/40–70/30. Highly to moderately separated subangular-subrounded blocky microstructure. Peds show subhorizontal internal fissures and frequent bio-reworking. Packing voids and bioturbation-related porosity. Calcitic crystallitic b-fabric. Coarse fraction random distribution. Heterometric rock fragments with dissolution traits. Mainly subangular limestone, calcitic crust and ophite fragments (≤5–6 cm). Quartz grains are predominantly angular and consist mainly of fine sands and silts. Angular medium-coarse quartz sand (≤2%). Coarse and fine subrounded–rounded silt (5% approx.). Very fine rounded sand (2% approx.). Abundant sediment aggregates rich in reddish clay with reworked iron nodules. Frequent microcrystalline calcitic concretions with detrital inclusions. Carbonate dissolution and recrystallisation traits on rock fragments and calcitic features. Carbonated root cells. Thick pendants alternating micritic and microsparitic layers. Fresh root and other plant tissue (≤2% − 500 μm approx.). Occasional fresh bone fragments (≤150 μm). Fe–Mn staining and nodules mainly in secondary position.
S1-20	Sterile Scattered Mousterian artefacts	CGM11 CGM11-13	Yellowish brown (7.5YR 5.6). Silty clay loam. 20–5 cm thick approximately discontinuous to the East. Fine-to-medium subangular and subrounded pebbles. Secondarily very coarse angular pebbles. Sharp lower boundary at the contact with S1-25 and S1-30. Sharp upper boundary at the contact with S1-10. Moderately sorted with discontinuous bedding. Scattered inclusions of comminuted charcoal and small bone fragments. Subrounded clasts with visible compacted, reddish calcitic pendents. Locally dispersed powdery secondary carbonates at the top.	Mainly mineral accumulation. cf ratio 63 μm 60/40–70/30. Highly to moderately separated subrounded blocky, granular and crumb microstructures. Subhorizontal fissures on sediment aggregates. Packing voids, bioturbation-related porosity. Vesicle porosity. Coarse fraction randomly distributed and occasionally verticalised including subangular and subrounded limestone, calcitic crust and ophite fragments (≤2.5 cm). Abundant reworked reddish sediment aggregates. The matrix is highly silty with inputs of sand and clay in which coarse to medium angular quartz sand is approximately ≤2% and coarse and fine subrounded-rounded silt is roughly ≤5%. Quartz grains are predominantly angular and consist mainly of fine sands and silts. Microcrystalline calcitic concretions and nodules, frequently with diffuse boundaries and impregnating the groundmass Layered pendants alternating micritic and microsparitic layers. Calcitic hypocoatings, micritic and microsparitic coatings and calcitic recrystallisation of detrital features as bone fragments. Black amorphous matter and bone tissue around coarse fraction and embedded in calcitic

				pedofeatures. Abundant reddish dusty clay coatings. Fe impregnations and dendritic Mn nodules in primary position. Iron-rich pedofeatues in secondary position. Frequent reworked features and sediment aggregates from anthropogenic origin randomly distributed. Unevenly burnt plant and bone tissue (300/500–3000 μm approx.)
S1-25	Reworked combustion residues + Mousterian artefacts	CGM12 CGM13 (top section)	Yellowish (7.5YR 6/4–6/6). Silty. 5–10 cm thick approximately. discontinuous. Gradual lower boundary. Sharp upper boundary. Increasing coarse geogenic fraction when compared to S1-30.	Organo-mineral accumulation. cf ratio 63 μm 20/80. Granular and crumb microstructures. Fissures in sediment aggregates and bioreworking. Packing voids, biochannels and local vesicular porosity. Crystallitic b-fabric. Coarse fraction randomly distributed. Subangular and subrounded limestone, calcitic crust and ophite fragments. Quartz grains predominantly angular and consisting of fine sands and silts. Angular quartz medium-coarse sand (≤2%). Coarse and fine subrounded–rounded silt (5% approx.). Sediment aggregates rich in quartz grains and clay lacking anthropogenic features. Traits of carbonate dissolution. Reworked ash lumps and sediment aggregates including charcoal, calcitic plant pseudomorphs and partially burnt bone fragments (≤500 μm) with reddish biogenic erosions. Burnt sediment aggregates (≤3 mm). Microcrystalline calcitic impregnation of the groundmass and micritic nodules with both diffuse and sharp boundaries. Pendants alternating dark micritic and light sparitic layers. Calcitic hypocoatings and micritic/microsparitic coatings. Abundant Fe–Mn staining. Iron-rich pedofeatues in secondary position.
S1-30 S1B	In situ combustion residues + Mousterian artefacts	CGM13 CGM14 CGM18	25 cm thick approx. Continuous layer. Scarce and subrounded coarse fraction. Whitish (7.5 YR 7/4) matrix. Clayey fine silts. Sharp lower boundary. Upper boundary: Gradual at the contact of S1-25 facies and sharp at the contact of S1-20 facies. Coarse fraction: ≤ 5%. Matrix partially cemented. Scattered and discontinuous convex-shaped black- brown (7.5YR 4/3) laminations 2–3 cm thick.	Ash layers: Common characteristics to all ash accumulations: Mineral groundmass. cf ratio 63 μm 2/98–5/95. Vughy with patches of granular-crumb microstructure. Porosity from soil fauna and plant bioturbation. Fissures at the top of the accumulations. Calcitic crystallitic b-fabric. Scarce quartz grains consisting of angular silts and fine sands. Scattered subrounded dark greyish and brown rock fragments showing fissural patterns from combustion (≤1 cm). Subrounded reddish sediment aggregates (≤4000 μm). Calcitic recrystallization of the groundmass including micritic hypocoatings and micritic and microsparitic coatings around pores. Increasing accumulation of subangular fresh rock fragments (≤3–4 cm) and biospheroids from soil fauna to the top of the accumulations. Scattered coprolithic residues (≤300 μm) at the top of the ash accumulation. Sharp lower boundary. Variable concentrations of the following remains are found in different ash lenses: a) Greyish patches with embedded yellowish amorphous accumulations and prismatic calcitic pseudomorphs anatomically articulated. b) Rounded calcitic pseudomorphs after oxalate druses often in clusters. c) Calcitic pseudomorphs after multicellular plant tissue (≤800 μm). d) Subrounded–rounded patches of micritic residue from strong combustion of bone tissue (≤3000 μm).associated with whitish burnt bone fragments (≤1 cm). Charred layers: Organo-mineral groundmass. cf ratio 63 μm 20/80. Vughy-subrounded-crumb microstructure. Coarse fraction randomly distributed. Burnt sediment aggregates (≤500 μm) and rock fragments (≤2.5 cm). Partially burnt bone fragments (≤1500 μm). Charcoal (≤500 μm). Subangular quartz. Biospheroids from soil fauna. Calcitic recrystallisation of the groundmass including micritic hypocoatings and micritic and microsparitic coatings.

S1-30 presents lateral continuity along the profiles of the Ramp sector. The top of this accumulation fades gradually into facies S1-25 (Fig. 4) although to the laterals S1-25 disappears and sharp contacts between S1-30 and S1-20 are detected. During the excavation, Mousterian artefacts from S1B level were consistently associated with the top of S1-30, however, towards the West, in the area investigated for this work, Mousterian pieces were also found embedded in S1-25, S1-20 and at the bottom of S1-10, suggesting partial reworking of assemblages from layer S1B (Fig. 3A).

S1-30 and S1-25 display similar fine-grained matrix content (<75%), although relevant differences between both facies have been recorded at macroscopic and microscopic level.

S1-30 shows greater vertical extension than S1-25, whitish/light gray colour (7.5 YR 7/4.) and a matrix partially cemented in which scattered and discontinuous 2–3 cm thick convex-shaped black laminations are observed. Thin section analysis indicates that sediments from S1-30 are mainly anthropogenic in origin and are made of overlapping combustion structures characterised by a layer of mineralised residues on top (ash) and an accumulation of partially burnt sediments at the bottom. Micromorphological results from three different samples (CG M13, CG M14 and CG M18) document lateral variability of S1-30 (Fig. 3A) and indicate a consistent presence of vegetal matter and bone tissue in the combustion residues throughout this accumulation (Table 1).

Differences in the relative proportion of plant and bone residues among the three samples studied are observed. Accumulations of calcitic prismatic pseudomorphs, which appear frequently interconnected and following linear patterns, have been recorded in the combustion remains from sample CGM13 (Fig. 6e and g). In sample CG M18 in contrast, rounded calcitic pseudomorphs from combustion of druse oxalates, frequently documented in clusters preserving the original arrangement of the oxalates in the plant tissue, are dominant (Fig. 6h). Interestingly, in this ash accumulation pseudomorphs after prismatic or rhomboedric oxalate crystals are very scarce.

Fresh wood contains prism and druse phytoliths made of calcium oxalate that can be distributed throughout the different anatomical sections of the plant tissue (Franchesci and Horner, 1980; Franchesci and Nakata, 2005). Experiments have shown that combustion transforms such plant biomineralisations into calcitic pseudomorphs as those identified in the samples from Cova Gran (Brochier, 1983; Canti, 2003; Alexandrovskii, 2007; Braadbaart et al., 2012).

Concentrations of calcitic pseudomorphs are frequently documented in sediments from archaeological contexts and are commonly referred to as wood ash (Courty et al., 1989). In thin section high proportions of calcitic pseudomorphs after prismatic and rhomboedric oxalate crystals are associated with the combustion of wood (Brochier, 1983; Wattez and Courty, 1987). Palaeobotanical data support the use of wood as relevant fuel choice in Iberian MP contexts (Albert et al., 2012; Vidal-Matutano et al., 2015). Although both prisms and druses oxalate can be found in ligneous tissue larger proportions of oxalate druses have been documented in leaf tissue (Brochier, 1996, 1999).

Consequently concentrations of pseudomorphs after oxalate druses as those detected in the combustion residues from sample CGM18, might be indicating the burning of leafy remains, or at least of plant tissue rich in this kind of plant biomineralisation, in relatively high proportions at Cova Gran.

To a lesser extent aggregates of long articulated silica phytoliths have also been recorded in the ash accumulations from facies S1-30 (Fig. 6f). Long silica phytoliths are commonly associated to grasses (Piperno, 1988) and the presence of specimens in anatomical conexion can be considered as an indicator of their preservation in primary position.

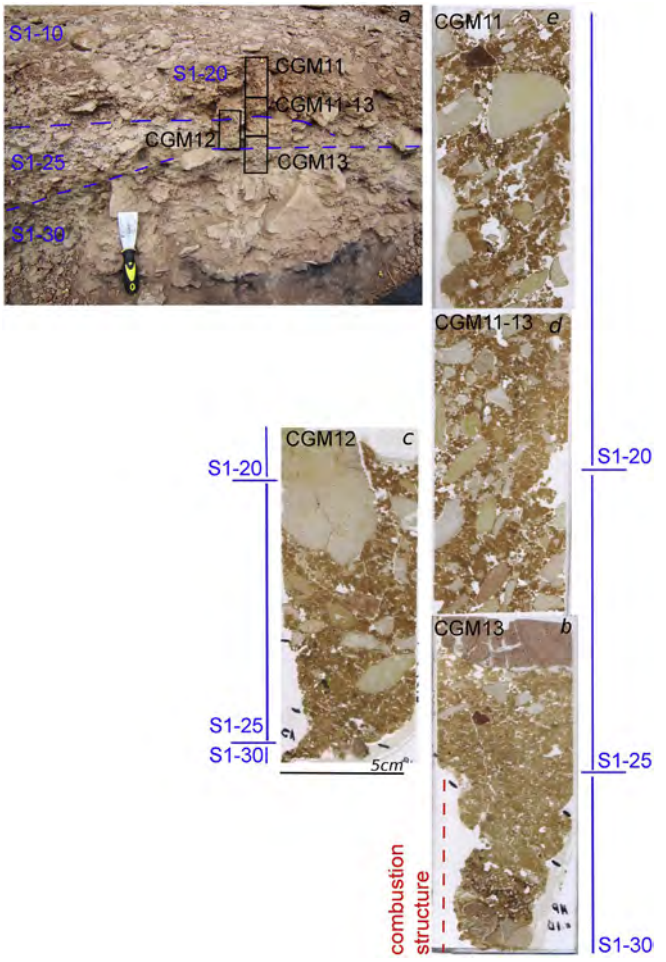

Fig. 5. a) MUP transitional sequence. Note stratigraphic contacts between facies S1-30, S1-25 and S1-20 and the location of samples for micromorphological analysis. b) – e) Scans of thin sections CGM13, CGM12, CGM11-13 and CGM11 and corresponding sedimentary facies and stratigraphic contacts from bottom to top. b) Thin section CGM13. Facies S1-30 and stratigraphic contact between S1-30 and S1-25. Note *in situ* combustion residues at the contact between S1-30 and S1-25. Note also gradual contact between facies and increasing input of geogenic debris to the top of the slide. c) Thin section CGM12. Contact between facies S1-25 and S1-20. Increasing input of geogenic debris can be observed. d), e) Thin sections CGM11-13 and CGM11. Facies S1-20. Note darker colour in thin section CGM11 as a result of increasing inputs of non-anthropogenic debris including translocated material from local soils. (For interpretation of the references to colour in this figure legend, the reader is referred to the web version of this article.).

In addition to plant remains bone residues consisting of greyish patches with rounded edges, microgranular structure, irregular porosity and reddish specks on the surface are commonly observed, especially in sample CGM14 (Table 1, Fig. 7e and g). Close-up views of these features reveal that are made of concentrations of micrite-sized crystals (Fig. 7h).

The effects of combustion on bone tissue have been addressed through experimental investigations. Results of these works show that direct exposure of fresh bone to temperatures ranging between 500 °C – 700 °C produces granular surfaces, rounded edges and alteration of vascular porosity that can be observed at microscopic level (Nicholson, 1993). These microscopic characteristics are expression of changes in bone crystal structure confirmed by SEM and infra-red spectroscopy analyses (Nicholson, 1993; Stiner et al., 1995). Scattered whitish grey bone fragments have also been observed in the same micro-sedimentary context where the grey patches described above

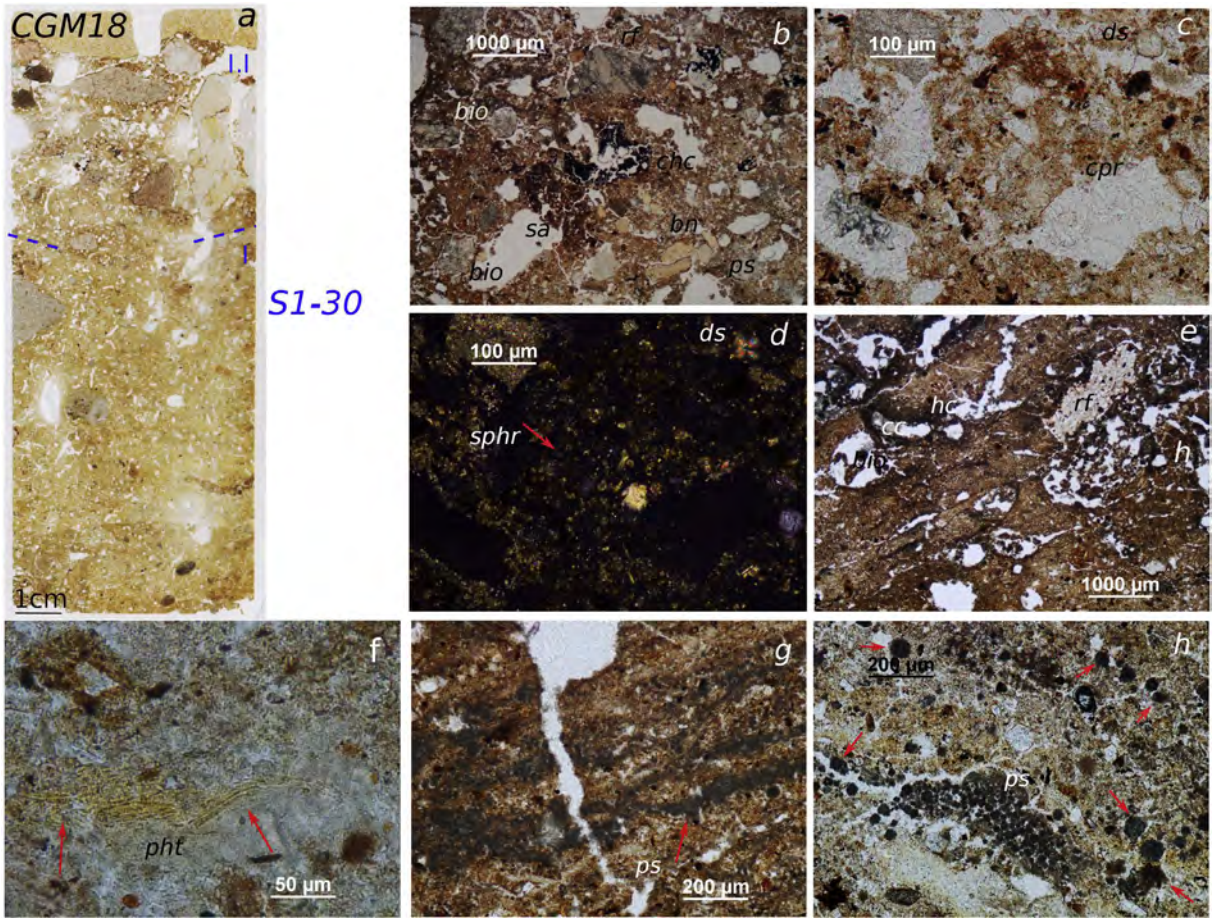

Fig. 6. Combustion residues from the top of the Mousterian sequence (facies S1-30). a) Scan of thin section CGM18. Note microstratification of sediments showing (I) *in situ* well preserved calcitic ashes and (I.I) reworked ashes from the underlying accumulation containing rock fragments and biogenic features as a result of surface exposure and soil fauna disturbance. b) – h) Microphotographs from slides CGM18 and CGM13. b) Thin section CGM18. Microfacies I.I. showed in a). General view of reworked ashes. Note weathered unevenly combusted anthropogenic and non-anthropogenic remains as charcoal (chc), charred bone (bn) and burnt sediment aggregates (sa) and calcitic pseudomorphs (ps) mixed with fresh (non-burnt) rock fragments (rf) and soil fauna biospheroids (bio). PPL. c) Thin section CGM18. Microfacies I.I showed in a). Coprolite aggregate from reworked ash layer. PPL. d) same view as in b) in XPL. Note faecal spherulites (sphr) and oxalate druses (ds) from plant remains embedded in the feature possibly corresponding to herbivore dung. e) Thin section CGM13. Phosphatised ash accumulation from combustion structure (see Fig. 5 b). Note compaction and homogeneous combustion of the groundmass with porosity related to faunal bioturbation (bio), geogenic inclusions (rf) and hypocoatings (ch) and coatings (cc) from calcitic recrystallisation. PPL. f) Thin section CGM18. Microfacies I. Ash layer. Long silica phytoliths in anatomical articulation likely from grass remains (arrows). PPL. g) Thin section CGM13. Wood ash from combustion structure (see Fig. 5 b). Detail of anatomically articulated pseudomorphs after unicellular oxalates (ps) in linear arrangement. PPL. h) Thin section CGM18. Microfacies I. Ash layer. Concentration of rounded calcitic pseudomorphs (ps) after oxalate druses in anatomical articulation (arrow). Note the same type of calcitic pseudomorphs throughout the matrix (arrows). PPL.

have been recorded (Fig. 7f). The colouring and optical properties in thin section of these bone fragments from Cova Gran match the characteristics of burnt bone observed in thin sections from experimental samples aimed to provide reference material for the study of combustion residues from Middle and Upper Palaeolithic contexts (Miller et al., 2010; Mallol et al., 2013a).

In addition greyish patches associated with intensively burnt bone fragments as recorded in samples from Cova Gran have been identified as the main components of bone ashes in Holocene incineration pits from the Iberian Peninsula. Micromorphological and microprobe analyses allowed optical and compositional characterisation of these residues (Polo-Díaz, 2010).

Rounded sub-millimetric reddish erosions on bone surface are the result of collagen digestion by microorganisms (Hackett, 1981). These features are characteristic alteration traits of human and faunal bone remains in archaeological contexts (Jacks et al., 2001; Jans et al., 2004; Polo-Díaz and Fernández Eraso, 2010).

Reddish specks similar to biogenic erosions have been consistently documented on burnt bone, as well as on the micritic greyish patches associated with them, in the samples from Cova Gran (Fig. 7e and h), which provides additional support for the characterisation of these greyish patches as bone residues.

Concentrations of intensively combusted bone residues in sample CGM14 are mixed with mineralised plant remains rich in druse pseudomorphs. Small rock fragments and sediment aggregates, also with evidence of combustion at high temperature (e.g. fissures and greyish brown colour), appear in the same microsedimentary context of mineralised plant residues. No indicators of secondary deposition or dumping dynamics (Schiegl et al., 2003) affecting either the bone residues or the sedimentary matrix have been observed.

The potential use of bone as fuel in Palaeolithic contexts and its possible implications in terms of social behaviour have been explored through experiments (Costamagno et al., 2005, 2009; Théry-Parisot and Costamagno, 2005).

Preliminary results on combustion residues of facies S1-30 from Cova Gran point to a possible use of bone as fuel during the Late MP occupation of the site. Systematic analysis of the MP combustion

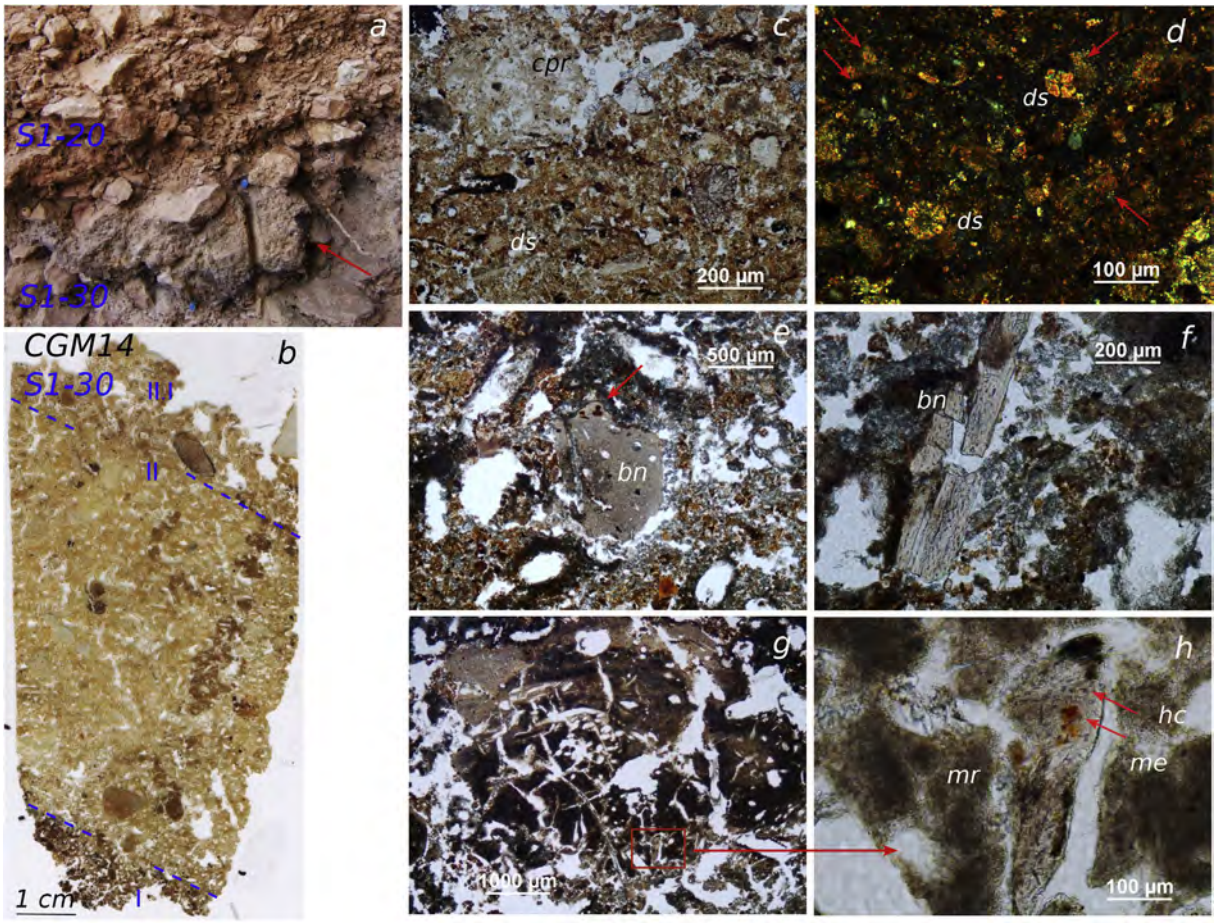

Fig. 7. Combustion residues from the top of the Mousterian sequence (facies S1-30). *In situ* combustion structure and block sample for micromorphological analysis in the profile (arrow). Note clear sedimentary change at the top of the combustion structure showing sharp contact between facies S1-30 and S1-20 in the westernmost area of the MUP transitional sequence (see also Fig. 3A). b) Scan of thin section CGM14 from sample showed in a). Note microstratification of residues: charred remains at the bottom of the slide (microfacies I) are overlain by well preserved ashes (microfacies II) and reworked ash residues from surface exposure at the top (microfacies II.I). Note sharp contact between I and II microfacies and homogeneous internal thermal alteration. c) – h) Microphotographs from thin section CGM14. c) Microfacies II.I. Coprolite (cpr) and plant remains including druses (ds). PPL d) Microfacies II.I. Detail of non-charred plant remains including druses (ds) and faecal spherulites (arrows). XPL. e) Microfacies II. Light grey strongly burnt subrounded bone fragment (bn). Note altered bone porosity and reddish specks from biological activity at the top of the feature (arrow). The feature is embedded in a recrystallised groundmass where frequent calcitic hypocoatings and coatings around voids are observed. PPL. f) Microfacies II. Whitish-light grey bone fragment (bn) strongly combusted but still preserving original morphology and porosity (haversian canals). PPL. g) Microfacies II. Bone fragment showing strong thermal alteration. PPL. h) Detail of red box in microphotograph g). Note grey micrite-sized granular surface (mr) and small whitish bone fragment still preserving original bone features as harvesian canals (hc). Reddish staining from microorganism activity (me) is also present. PPL. (For interpretation of the references to colour in this figure legend, the reader is referred to the web version of this article.).

remains from the deposit is currently in progress and will provide further insights into fire management at the site during this period.

Grain size distribution of layer S1-30 displays a main peak at 14.9 µm and a secondary peak at 0.3 µm (Fig. 4B), which supports field observations and characterisation in thin section of the accumulation as clayey silts.

Quartz morphoscopy in S1-30 is very hereteogenous, including some rounded particles. However, angular and very angular morphologies prevail indicating local sources of detrital inputs and minimising the possible role of allochtonous sedimentary agents, as wind or water dynamics, in the accumulation of debris. These results are in agreement with micromorphological observations. Quartz grains documented in thin section from bedrock fragments, sediment aggregates and matrix present similarities in angularity and size (i.e. mainly fine sands and silts) (Table 1).

Similar compositional, microstratigraphic and grain size patterns are observed from top to bottom in facies S1-30, which indicate similar sedimentary dynamics involved in the formation processes of the whole accumulation.

WDXRF analysis in S1-30 shows high content in CaO (37–40%), followed by SiO_2 (18.9–16.5%), Al_2O_3 (5.6–4.5%) and Fe_2O_3 (2.7–2%) (Table 2).

Table 2
Results of WDXRF analysis. Chemical composition of samples from facies S1-10 and S1-30.

WDRXF Sample	SiO_3 %	Al_2O_3 %	Fe_2O_3 %	MnO %	MgO %	CaO %	Na_2O %	KO_2 %	TiO_2 %	P_2O_5 %	SO_3 %	LOI %
S1-10 top	33.85	8.74	4.07	0.09	4.84	23.03	0.31	0.6	0.57	0.66	0.1	22.14
S1-10 bottom	34.31	8.55	3.94	0.09	4.42	23.21	0.3	0.59	0.57	0.7	0.07	22.25
S1-30 top	16.34	4.5	2.02	0.05	1.56	40.26	0.17	0.87	0.3	1.07	0.08	32.79
S1-30 bottom	18.82	5.64	2.67	0.07	2.24	36.76	0.25	0.87	0.42	1.27	0.17	30.83

High quantity of CaO in the compositional data from S1-30 is in agreement with micromorphological identification of calcitic ashes from plant tissue as a major agent of accumulation of carbonates in this facies. In addition calticic recrystallisations linked to post-depositional fluctuations in the environmental moisture levels illustrate the interrelation between anthropogenic and natural dynamics in the build-up and redistribution of carbonates in the sediments from this facies.

Significant percentages of Si, Al and Fe have also been documented in S1-30 (Table 2). Such values can be related to sediment aggregates which accumulation in well preserved calcitic ash layers can be linked to debris attached to plant tissue prior to combustion (Schiegl et al., 1996; Karkanas et al., 1999; Weiner et al., 2002). Microscopic observations of the sediments from Cova Gran indicate the presence of reddish brown (in the web version) sediment aggregates in the ash microfacies containing inclusions of quartz grains and limestone and ophite fragments in a clayey matrix (Table 1. Fig. 8a and b). Aggregates of opal phytoliths contribute also to the total amount of Si in the sediment.

Excremental residues from dung, guano and carnivore coproliths as well as from bone remains and their alteration by-products constitute the main source of phosphatic features in cave and rock-shelter prehistoric deposits (Goldberg and Nathan, 1975; Wattez et al., 1990; Weiner et al., 1993; Macphail et al., 1997; Karkanas et al., 2000, 2002; Shahack-Gross et al., 2004; Polo-Díaz, 2010).

In Cova Gran phosphate concentrations in samples from facies S1-30 are higher (1.0–1.2%) than those observed in samples from the sterile deposit (0.7–0.6%) (Table 2). Microscopic observations of sediments from S1-30 indicate that bone remains with variable degree of combustion and burnt phosphatised plant remains are the main sources of phosphatic materials. In addition patches of excremental residues recorded at the top of this facies also contribute to the total concentration of phosphates in the sediments.

Organic matter estimations provided by LOI are between 31 and 33% (Table 2). These values are considerably higher than those yielded by the overlying sterile deposit (22.1–22.2%) and are especially relevant since the original organic fraction from S1-30 has undergone major thermal alteration and ashes constitute the main detrital residue preserved. To a great extend the organic content of S1-30 is concentrated in the 2–3 cm thick black-brown (7.5YR 4/3) discontinuous laminations interspersed with clean ashes (Table 1). However, even in these blackish brown layers from Cova Gran the total amount of charcoal, charred bone and black amorphous organic matter is overweigh by partially combusted mineral-rich sediment aggregates and rock fragments. These features are embedded in a matrix with evidence of bioturbation occurring after combustion, but interestingly, also before combustion (Fig. 8c and d). The latter evidence indicates exposure of sediments to surface conditions before fire setting up.

Recent investigations on experimental and archaeological MP combustion structures provide a plausible explanation for such sedimentary pattern, suggesting that black accumulations underlying ash layers can be related not to fuel remains, but to debris from previous or synchronic occupation surfaces instead (Mallol et al., 2013b).

Concerning the taphonomy of the combustion residues from facies S1-30, physico-mechanical reworking (i.e. plant growth and soil fauna activity) has been documented in the charred microfacies, as well as in the mineralised accumulations. In addition, strong recrystallisations from redistribution of carbonates have been detected locally in the ashes (Fig. 6e). Scattered yellowish isotropic patches resembling apatite from bone diagenesis (Karkanas and

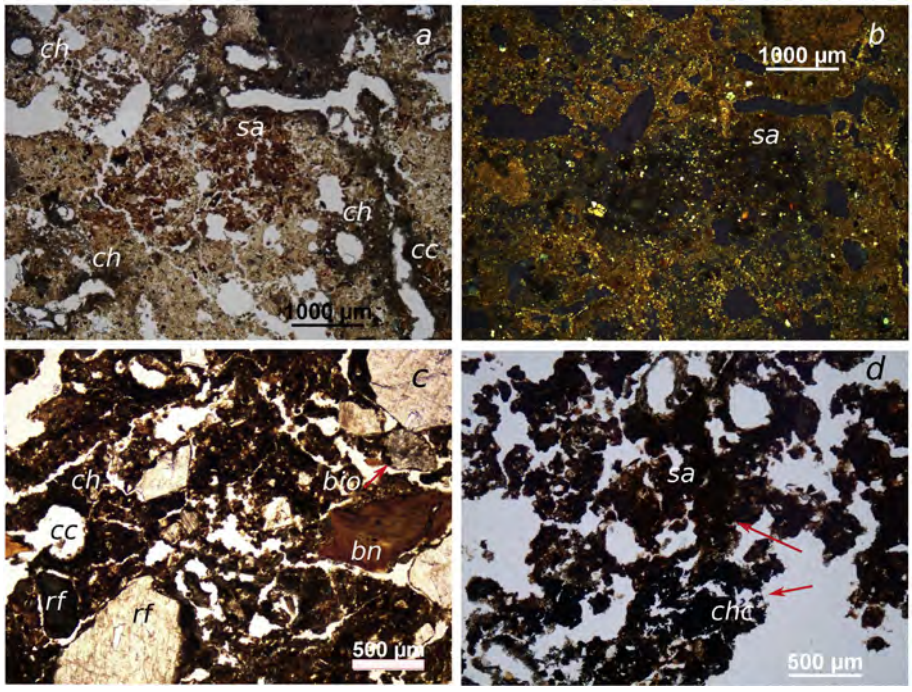

Fig. 8. Combustion residues from the top of the Mousterian sequence (facies S1-30). a) Thin section CGM18 (see Fig. 6a). Microfacies I. *In situ* ash layer. Subrounded sediment aggregate showing reddish brown clayey matrix (sa). PPL. b) same image as in a) in XPL. Note quartz grains and rock fragments inclusions in the feature. c) Thin section CGM13 (see Fig. 5b). Charred microfacies. Groundmass showing sediment aggregates rich in carbonised particles, charred bone (bn) and burnt rock fragments (rf). Note burnt soil fauna biospheroid (bio). Thermal alteration of the feature indicates exposure of sediments to surface conditions prior combustion. Note also abundant calcitic hypocoatings (ch) and coatings (cc) around pores, likely from dissolution and recrystallisation of ash. PPL. d) Thin section CGM14. Microfacies I. Reworked charred accumulation showing sediment aggregates (sa) and charcoal fragment (chc). PPL.

Goldberg, 2010) have been recorded. Otherwise, the calcitic plant-derived residues from S1-30 are well preserved suggesting the absence of major diagenetic dynamics affecting the sediments (Schiegl et al., 1996).

Microstratigraphic patterns observed in archaeological and experimental combustion features have shown that clear stratification and homogeneous internal thermal alteration in microfacies of burnt residues can be considered evidence of combustion structures preserved in primary position (Wattez, 1992; Berna and Goldberg, 2008; Miller et al., 2010).

Combustion residues from Cova Gran present sharp contacts between ash and charred layers as well as homogeneous internal thermal alteration of microfacies (Figs. 5b, 6a, 7b).

In addition the abundance of pseudomorphs preserving the arrangement of the plant original biomineralisations, as observed in the ashes from S1-30, is an indicator of undisturbed combustion remains (Mentzer, 2014) and confirms the hypothesis raised during fieldwork suggesting that this facies is the result of overlapping *in situ* hearths.

Increasing postdepositional *in situ* reworking (i.e. plant growth and soil fauna activity) and non-anthropogenic detrital input are observed to the top of the combustion structures from S1-30 (Figs. 6a and 7b). Here traits of human activity showing variable degree of combustion such as charcoal, bone and ash are mixed with rock fragments and biogenic residues from soil fauna with no evidence of combustion (Fig. 6b) as well as with excremental residues associated with plant remains (Figs. 6c,d and 7c,d).

Earthworm excreta (i.e. calcitic biospheroids) as those documented at the top of the MP combustion structures in Cova Gran are considered indicators of surface exposure in relatively stable environments (Becze-Deák et al., 1997).

The presence of these features in S1-30 in addition to the lack of sharp erosive contacts or traits related to high-energy sedimentary dynamics at the top of this facies indicate exposure and slow burial of the Late MP sediments and indicate a discontinuity in the accumulation of anthropogenic debris.

4.1.2. Facies S1-25

Facies S1-25 directly overlies S1-30, showing a gradual lower stratigraphic contact and limited lateral continuity when compared to the latter. Macroscopic features of facies S1-25 also reveal local lenticular geometry and enrichment of yellowish red chroma (7.5YR 6/6-6/8) of a matrix mostly silty (Table 1). At microscopic level, although traits related to human activity (e.g. ash aggregates, charcoal and charred bone fragments) are abundant, increasing reworking of the matrix (Fig. 9c) and inputs of non-anthropogenic debris (e.g. clay-rich sediment aggregates, fragments of calcitic crust and subrounded and subangular rock fragments) (Fig. 9a) are also observed towards the upper section of the facies (Fig. 9c).

Calcitic impregnation of the groundmass in the form of diffuse orthic nodules and hypocoatings and coatings, as well as development of desiccation fissures, are also observed (Fig. 9b). These features are in agreement with lenticular geometry observed at macroscopic level and are indicative of moisture fluctuations in the sediment (Durand et al., 2010).

The contact between S1-30 and S1-25 shows a gradual change in the accumulation between both facies (Fig. 5b). No erosive discontinuities or indicators of high-energy sedimentary dynamics are observed at this point of the sequence.

This evidence in addition to the presence of Mousterian artefacts in this facies, indicate that surface exposure dynamics observed at the top of S1-30 had continuity and resulted in the partial reworking of the upper section of the MP occupation area and the formation of S1-25. Such traits reinforce the hypothesis of discontinued human activity at this point of the sequence and are in agreement with an abandonment of the site.

4.2. The sterile deposit between the Late MP and the Early UP layers: facies S1-20 and S1-10

The sterile deposit between the Late MP and the Early UP layers at Cova Gran consists of two successive accumulations displaying distinctive sedimentary traits.

4.2.1. Facies S1-20

Facies S1-20 is a dry yellowish brown (7.5YR 5.6) deposit with lateral continuity and a variable thickness ranging between 5 and 25 cm approximately. The matrix is silty with inputs of sand and clay in which angular coarse to medium quartz grains are approximately $\leq$2% and coarse and fine subrounded–rounded silt is roughly $\leq$5%. S1-20 overlies S1-25 at the centre of the area studied, although to the sides it rests directly on S1-30, showing sharp boundaries at the contact with the anthropogenic sediments (Figs. 3A and 7a). S1-20 presents a wegde-shaped geometry, disappearing towards the east of the Ramp sector, probably eroded by its upper contact with S1-10. Sediments from S1-20 are moderately sorted with discontinuous bedding, including scarce matrix and subrounded clasts.

Reworking by soil fauna and scattered inclusions of charcoal and small bone fragments were observed in the field. The coarse fraction is composed of fine-to-medium subangular and subrounded pebbles, as well as very coarse angular pebbles. Compacted, reddish calcitic pendants are consistently observed below the coarse fraction. Dispersed secondary carbonates at the top of the accumulation are also documented.

Under the microscope (Table 1) this facies presents a mixture of highly to moderately separated subrounded blocky, granular and crumb microstructures with frequent subhorizontal desiccation fissures on sediment aggregates. Such sediment aggregates are very often complex reworked features consisting of clay-rich microaggregates containing quartz sand and silt inclusions as well as small limestone fragments (Fig. 9d and e).

The coarse fraction in S1-20 is randomly distributed including medium and coarse subangular and subrounded limestone, ophite and calcitic crust gravels (Fig. 5c–e). The rock fragments present layered pendants with alternating micritic and sparitic layers (Fig. 9f). Microcrystalline calcite concretions with evidence of dissolution and recrystallisation dynamics and diffuse calcitic nodules impregnating the sediment aggregates are frequent (Fig. 9g). Micritic hypocoatings are common around pores (Fig. 9h) in which cytomorphic crystals also occur. Recrystallisation of detrital features as bone fragments is also documented. Fe–Mn hypocoatings, coatings, impregnations and nodules are common, the latter showing both diffuse and sharp boundaries (Fig. 9i). Such pedogenic traits in S1-20 suggest a break in the sedimentation and soil development in an environmental context with contrasting humidity levels.

Impregnative redoximorphic features as those observed in S1-20, suggest periods of water saturation of the sediment for relatively short periods of time (Bouma et al., 1990; Boixadera et al., 2003; Lindbo et al., 2010). Desiccation cracks and abundant traits of carbonate dissolution and redistribution indicate moisture fluctuations in environmental conditions ranging from temperate to arid. Calcitic pendants have been reported in stony temperate to arid environments, while calcite coatings and orthic nodules have been related to soils with semiarid-temperate conditions (Durand et al., 2010). Hypocoatings are associated with arid to ustic soils subjected to fluctuations of the water table (Durand et al., 2010) and dissolution of calcitic features have been identified in

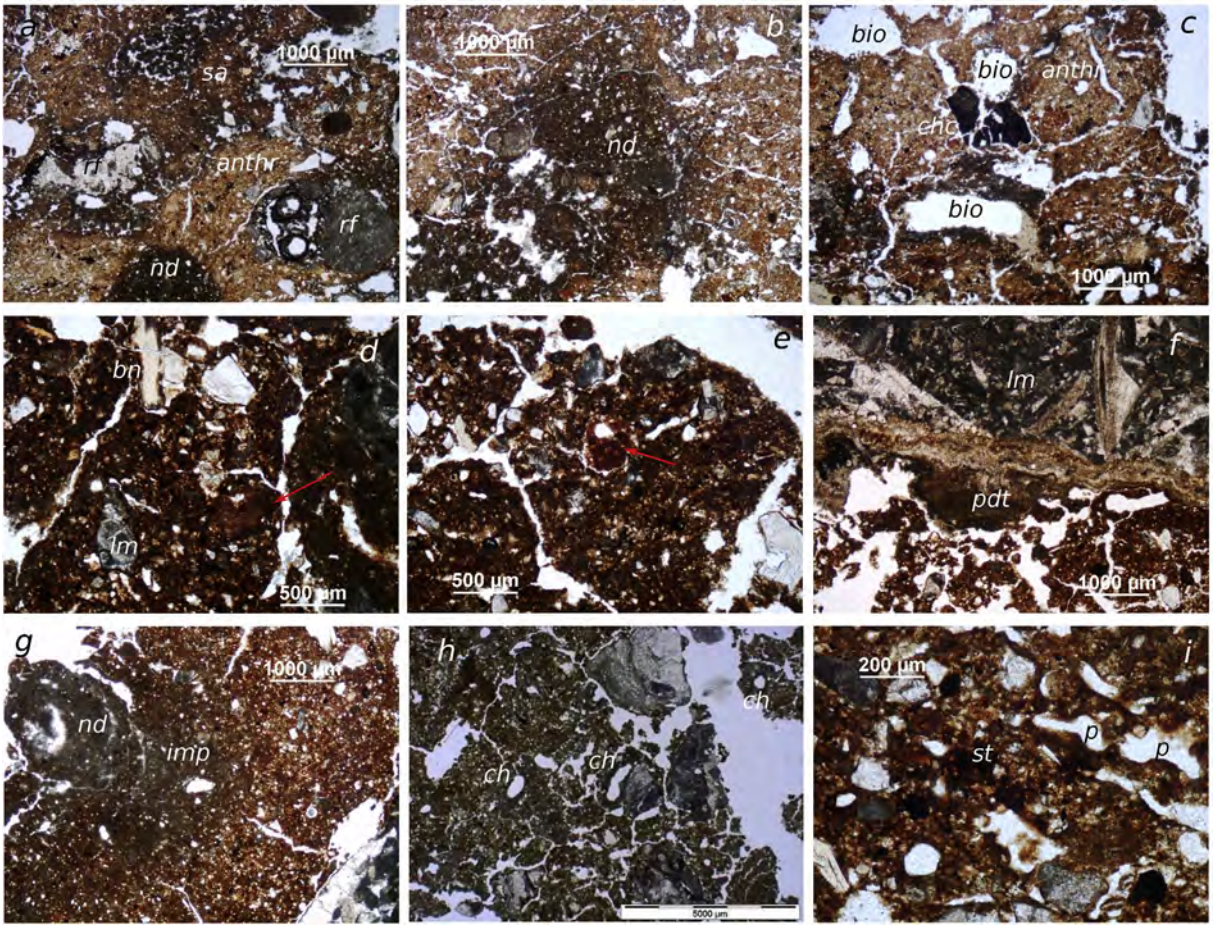

Fig. 9. Microphotographs showing sedimentary features from facies S1-25 and S1-20. a) facies S1-25. Thin section CGM13 (see Fig. 5b). Reworked anthropogenic sediment aggregates (e.g. anthrp). Note the features are in the same sedimentary context of non-anthropogenic debris: rock fragments (rf), sediment aggregates (sa) and calcitic nodules (nd). PPL. b) Facies S1-25. Thin section CGM13. Matrix strongly impregnated in calcium carbonate. Note sub-horizontal fissures in the groundmass from desiccation. PPL. c) Layer S1-25. Thin section CGM M12 (see Fig. 5c). Complex groundmass consisting of reworked anthropogenic sediment aggregates (anthr) and charcoal (chc). Note porosity related to bioturbation (bio) from soil fauna activity and plant growth. PPL. d) Facies S1-20. Thin section CGM11-13 (see Fig. 5d). Complex reworked sediment aggregate containing limestone (lm) and non-burnt bone (bn) fragments as well as subrounded red clayey sub-aggregate (arrow). LPP. e) Facies S1-20. Thin section CGM11-13. A further example of complex reworked sediment aggregate. Note reddish clayey inclusion of reworked soil (arrow). LPP. f) Facies S1-20. Thin section CGM11-13. Layered calcitic pendant (pdt) below a limestone fragment (lm) with alternating dark micritic and light microsparitic layers. PPL. g) Facies S1-20. Thin section CGM11-13. Partially dissolved and recrystallised micritic nodule (nd) and calcitic impregnative pedofeature (imp). Note sub-horizontal fissures in the groundmass. PPL. h) Facies S1-20. Thin section CGM11-13. Calcitic hypocoatings around biogenic pores (ch). PPL. i) Facies S1-20. Thin section CGM11-13. Fe–Mn staining (st) and coating and hypocoatings around pores (p). Note vesicular porosity. PPL. (For interpretation of the references to colour in this figure legend, the reader is referred to the web version of this article.).

palaeosoils sustaining changes from dry to humid conditions (Fedoroff et al., 2010).

The presence of local secondary carbonates at the top section of S1-20, provides further support to the hypothesis of a break in the sediment accumulation and subsequent soil development under arid to semihumid conditions (Gocke et al., 2012).

Sediment aggregates rich in clay and reworked pedofeatures are ubiquitous in S1-20 as mentioned above and reflect translocation of soil materials (Fig. 9d and e). In parallel vesicular porosity that can be related to muddy debris flows (Bertrand and Texier, 1999) is commonly observed in the groundmass (Fig. 9i).

As detailed in Section 2.1. Cova Gran is located at the bottom of a ravine, directly below a cliff 150 m deep (Fig. 10). In an scenario of moisture saturation of local sediments and soils, accumulation into the site of weathered materials from the top of the scarpment, could be favoured by the geomorphological setting of the rock-shelter. Gentle dipping of S1-20 towards the east (Fig. 3A) support the hypothesis that flows from the immediate context of the site entered the rock-shelter from above and/or from the western lateral of the Ramp sector. Although partly eroded by S1-10, facies S1-20 shows progressive wedging towards the east which suggests decreasing energy and incidence of slope dynamics in the underlying archaeological deposit. The presence of reworked sediment aggregates rich in translocated soil material and associated vesicular porosity together with coarse fraction with traits of local displacement point to sedimentary inputs from the near sedimentary and soil context of the rock-shelter. Moderate sorting with discontinuous bedding, including scarce matrix and subrounded clasts in the westernmost area of the Ramp sector is most likely related to water currents coming from the west during periods of increased environmental humidity.

Mousterian artefacts were found in the sedimentary unit S1-20 (Fig. 3 A). Microscopic observations of thin sections from this facies reveal the presence of scattered reworked features from anthropogenic origin in the same sedimentary context where dispersed artefacts were recorded. Mineral features with optical properties resembling flint fragments (Angelucci, 2010) together with fresh and heterogeneously burnt plant and bone fragments appear in secondary position and randomly distributed in a groundmass rich in rock fragments, calcitic crust and reddish sediment aggregates

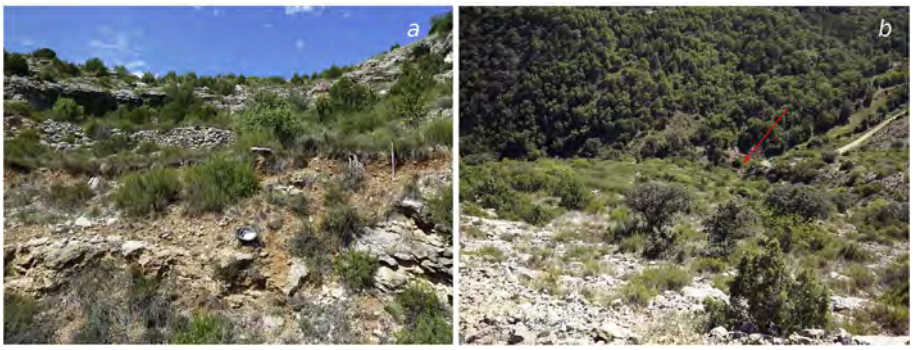

Fig. 10. a) View of the upper section of the cliff above Cova Gran. Note sediment and soil materials on the slope. b) View of the lower section of the cliff and location of the site at the bottom of the Sant Miquel ravine (arrow).

(Fig. 11a–f; see also Fig. 9d–i for sedimentary context of anthropogenic features showed in Fig. 11).

Such sedimentary traits suggest that the occurrence of anthropogenic features documented in S1-20 is the result of partial reworking of sediments from the underlying facies S1-25 and S1-30. It also implies that natural sedimentary dynamics are in the origin of the partial redistribution of combustion residues and artefacts observed at the top of the MP sequence in the area studied.

Fabric analysis has proven to be a reliable tool for assessing the integrity and the effects of reworking and slope dynamics in the

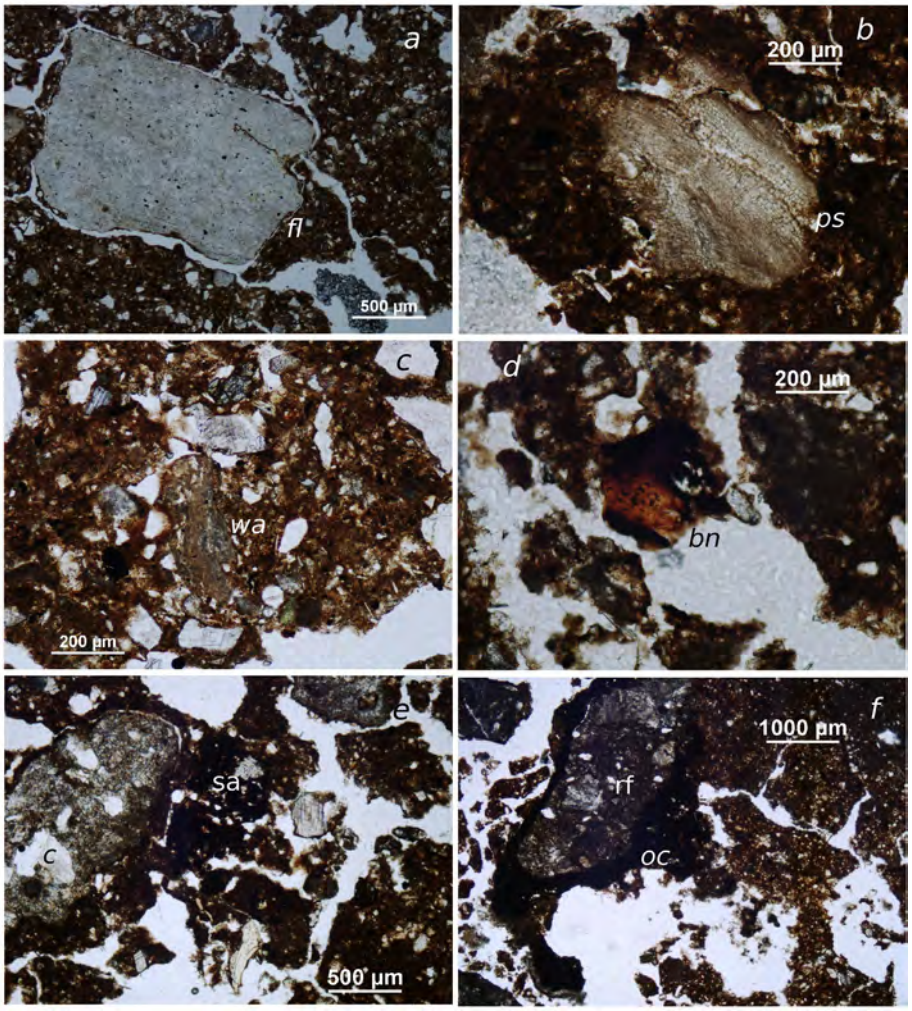

Fig. 11. Facies S1-20. Microphotographs of reworked anthropogenic features. a) Thin section CGM11-13 (see Fig. 5e). Flint fragment (fl). Note smooth edges from reworking. LPP. b) Thin section CGM11 (see Fig. 5d). Calcitic pseudomorph preserving plant multicellular structure (ps). PPL. c) Thin section CGM11-13. Verticalised lump of wood ash (wa). PPL. d) Thin section CGM11. Charred bone fragment (bn). PPL. e) Thin section CGM11. Concentration of carbonised matter in reworked sediment aggregate (sa). Note calcitic recrystallisation to the left of the feature (c). PPL. f) Thin section CGM11. Reworked rock fragment (rf) with organic coating (oc). PPL.

archaeological record (Bertrand and Texier, 1995; Lenoble and Bertran, 2004; McPherron, 2005; Lenoble et al., 2008). Analysis of orientation, dip angles and vertical distribution of bone, lithic artefacts and geogenic clasts from layer S1-B in Cova Gran as well as from experimental fabrics indicate homogeneous sedimentary patterns in agreement with *in situ* preservation of occupation surfaces (Benito-Calvo et al., 2009, 2011; Roy et al., 2014) (Fig. 2C). These data are consistent with the geoarchaeological evidence presented in this work which indicates limited incidence of natural dynamics on combustion residues and artefacts at the top of the MP sequence.

Sharp upper boundaries displayed by S1-20 suggest subsequent degradation dynamics affecting this accumulation with scours cutting down into the sediments from facies S1-10. Such processes resulted in partial erosion and truncation of S1-20 towards the east of the deposit (Fig. 3A).

At microstratigraphic scale a clear change is observed in thin sections between facies S1-20 and S1-10 providing further support to the hypothesis of a shift in the sedimentary dynamics between both accumulations (Fig. 12).

4.2.2. Facies S1-10

Facies S1-10 is a clast-supported breccia, very poorly sorted, massive and heterometric. This accumulation is characterised by a reddish-brown (5YR 6/4) loamy matrix (35–50%) rich in angular limestone clasts (65–50%) which show a tendency to platy patterns and horizontal arrangement (Table 1). The accumulation presents lateral continuity and a variable thickness with visible charcoal fragments, aggregates from soil fauna activity and small fragments of bone.

Under the microscope the coarse fraction is randomly distributed and consists mainly of limestone, calcitic crust and ophite fragments. In contrast to S1-20, geogenic inputs present more marked subangular and heterometric patterns and traits of calcitic dissolution and recrystallisation (Fig. 12).

Microstructure is highly to moderately separated subangular-subrounded blocky with bioturbation from plant growth and soil fauna activity. The groundmass of S1-10 includes reworked sediment aggregates rich in reddish clay and pedofeatures in secondary position as in facies S1-20 (Fig. 13a and b). Development of subsequent desiccation cracks is also observed in sediment aggregates as in the underlying accumulation (Fig. 13c).

Calcitic features present similarities but also significant differences from those observed in S1-20. Concretions of microcrystalline calcite with detrital inclusions are larger and more abundant than those observed in S1-20. These features are also affected by more intense dissolution and recrystallisation dynamics (Fig. 13d).

In contrast to sediments from facies S1-20, micritic diffuse nodules and hypocoatings impregnating the groudmass are not observed in S1-10.

Layered pendants are present in the lower part of the coarse fraction as recorded in S1-20. However, in S1-10 pendants are whitish and friable as documented during fieldwork. Their frequency is also higher than in S1-20 and markedly thicker with alternating dark micritic and light microsparitic - sparitc layers (Fig. 13e and f). Microsparitic recrystallisations and cytomorphic cells from calcified roots are also observed (Fig. 14a). Calcitic recrystallisations are lacking on scattered detrital particles in contrast to S1-20. Inherited redoximorphic features are abundant, however, their concentration in primary position tends to be lower than in S1-20 and iron hypocoatings and coatings are seldomly observed in the pores.

Accumulation of angular and heterometric debris from mechanical disaggregation of the parent material, as documented in facies S1-10 from Cova Gran, is characteristic of the coarse fraction in cave and rock-shelter deposits of the Mediterranean rim (Woodward and Bailey, 2000; Woodward and Goldberg, 2001). Cryoclastism is considered an important triggering dynamic in the accumulation of rock debris in karstic environments in general (Ford and Williams, 2007) and in cave and rock-shelter Palaeolithic contexts in particular (Laville, 1976; Laville et al., 1980). According to this interpretation, previous sedimentary characterisation of facies S1-10 from Cova Gran suggested the incidence of freezing and thawing cycles in the accumulation of the angular coarse fraction (Benito-Calvo et al., 2009). Microscopic observations currently available provide further insights into this question. No clear evidence of frost dynamics have been documented in thin section. Indicators of such dynamics as platy/lenticular microstructures, silt cappings or fissured/fractured coarse fraction (Van Vliet Lanöe, 1987, 1998) are absent from the sedimentary record. In contrast, traits of wetting–drying processes are common in the sediments in the form of desiccation cracks, enhanced porosity of limestone fragments and cyclical dissolution and recrystallisation of carbonates.

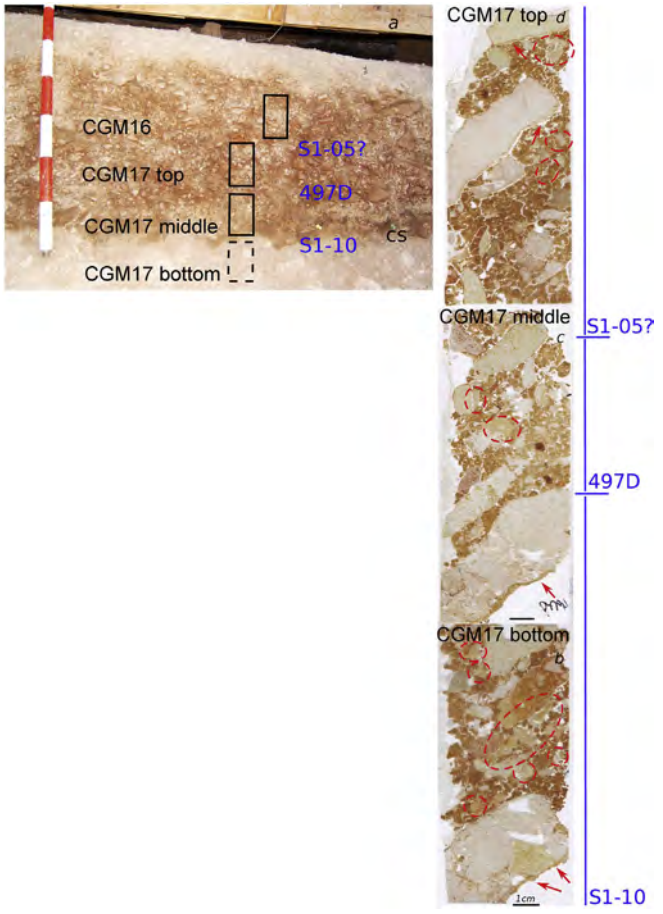

Fig. 12. a) MUP transitional sequence in the Ramp sector. North section. Location of samples for micromorphological analysis documenting facies S1-10 and layer 497D. Slides from samples collected above level 497D, possibly corresponding to S1-05, are also included. Note in situ combustion structure (cs) in level 497D adjacent to block sample CGM17 middle. b) Facies S1-10. Scan of thin section CGM17 bottom. Note abundant coarse fraction and whitish calcitic concretions (red circles) from carbonate redistribution in the matrix. Layered calcitic pendants are visible below the limestone fragments (arrows). c) Level 497D. Scan of thin section CGM17 middle. Note accumulation of light sediment aggregates from anthropogenic origin at the centre of the slide. d) Scan of thin section CGM17 top possibly corresponding to facies S1-05. Note sedimentary traits similar to those observed in sample CGM17 bottom. (For interpretation of the references to colour in this figure legend, the reader is referred to the web version of this article.).

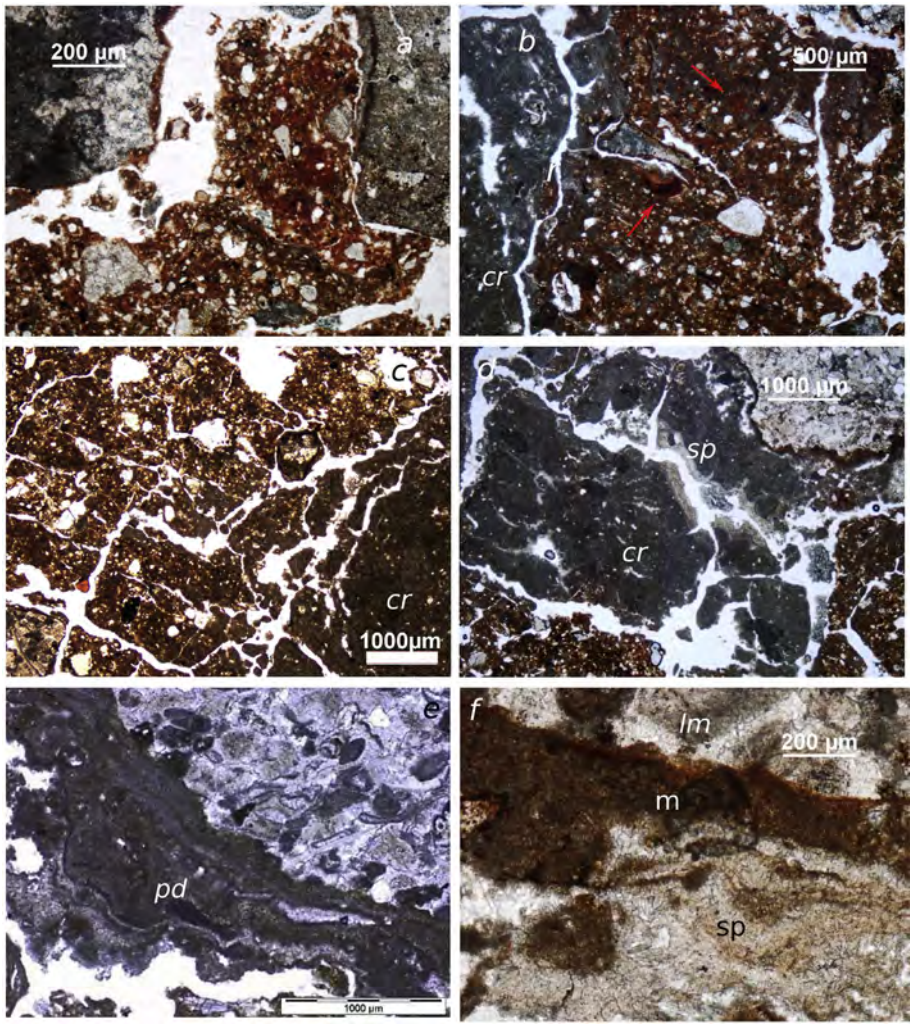

Fig. 13. Microphotographs from facies S1-10. Thin section CGM17 bottom (see Fig. 12b). a) Sediment aggregates rich in clayey reddish patches likely from soils in the immediate area of the site. PPL. b) Reworked iron-rich soil pedofeatures (arrows). PPL. c) Groundmass affected by desiccation. Note sub-horizontal fissures on sediment aggregates and micritic calcitic concretion to the right (cr). PPL. d) Polygenetic calcitic feature. Microcrystalline calcitic soft concretion (cr) with desiccation fissures and traits of successive dissolution and microsparitic recrystallisation (sp). PPL. e) Calcitic pendant (pd) alternating dark micritic and light microsparitic layers below a limestone fragment. PPL. f) Detail of a calcitic pendant below a limestone fragment (lm) showing dark micritic (m) and light microsparitic (sp) layers. PPL.

Moisture fluctuations have also been addressed as relevant dynamics involved in the alteration and weathering of bedrock structure (Farrand, 1975; Collcut, 1979). Such fluctuations could have caused swelling and shrinking stress on the bedrock surface of Cova Gran leading to progressive disaggregation of the wall and roof structures of the rock-shelter and favouring accumulation of angular and subangular slabs in the deposit.

Carbonate pedogenesis as described above supports the incidence of contrasting humidity oscillations.

Cytomorphic calcite is associated with climatic patterns in which long dry seasons prevail (Becze-Deák et al., 1997). Intense calcitic dissolution and recrystallisation dynamics as those observed in S1-10 suggest fluctuations from dry to humid conditions (Fedoroff et al., 2010).

Thick pendants are associated to relatively arid environments (Khokhlova et al., 2001; Khormali et al., 2006). Alternating dark micritic and light microsparitic layers have been used as an indicator of palaeoclimatic fluctuations and associated changes in biological activity linked to environmental moisture. Light microsparitic crystallisations have been related to periods with relatively higher aridity and decreased biological activity. In contrast dark organic-rich micritic crystallisations have been related to periods with higher moisture availability favouring plant growth and faunal activity (Durand et al., 2010).

Carbonate pedogenesis takes place during periods of biostasy (Verrecchia, 2002). Therefore development of calcitic pedofeatures can be considered as an indicator of relatively stable surface conditions favouring biological activity and plant growth.

Concentration of root tissue and voids preserving organic plant-derived lining together with calcitic biospheroids and lumps of needle-fiber calcite from plant growth, soil fauna and biological activity respectively have been recorded throughout facies S1-10 (Fig. 14b and c).

Such features have been reported as indicators of organic matter accumulation during periods of relatively stable surface conditions in environments with contrasting humidity levels (Ould and Bruand, 1994; Becze-Deak et al., 1997; Verrechia and Verrechia, 1994; Khormali et al., 2006; Manafi and Poch, 2012). Accordingly, biological activity and carbonate pedogenesis documented in facies S1-10 from Cova Gran can be considered indicative of palaeosurfaces occurring during the formation of this facies in a general environmental context characterised by moisture fluctuations.

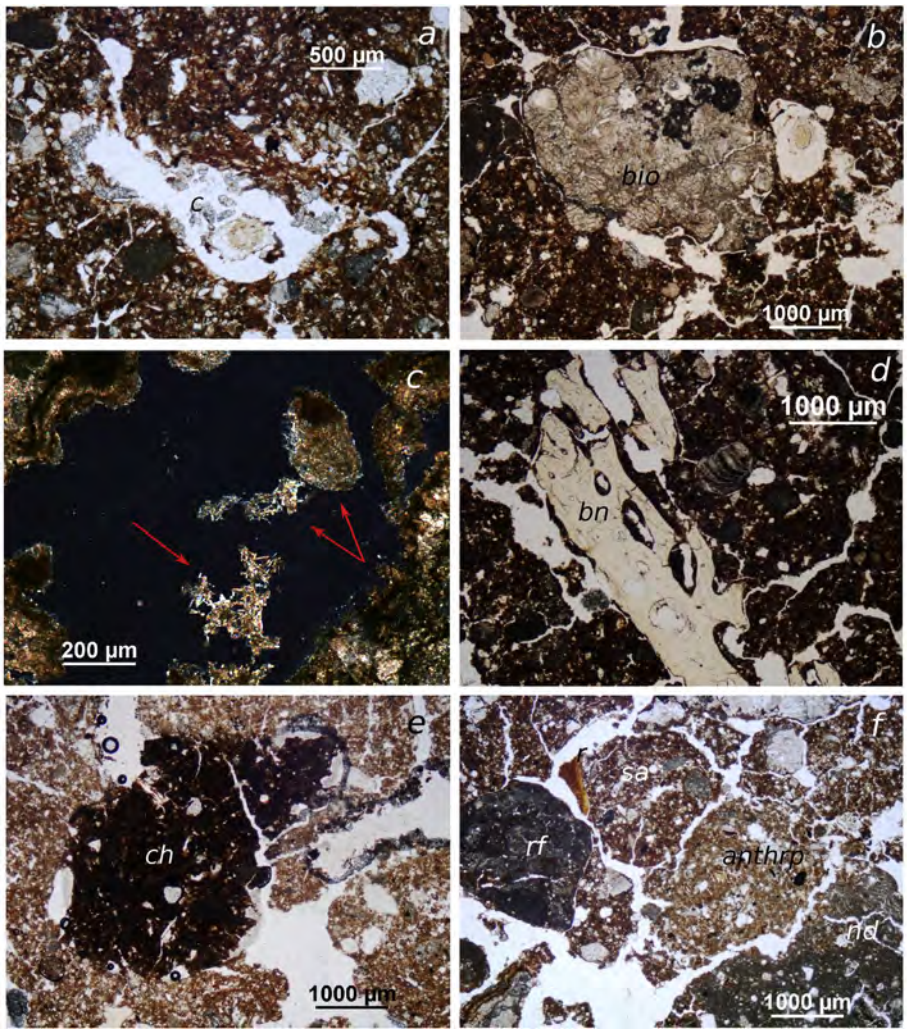

Fig. 14. Microphotographs from facies S1-10 and layer 497D. a) Thin section CGM17 bottom (see Fig. 12b). Cytomorphic calcite crystals in root channel (c). PPL. b) Thin section CGM17 bottom. Cluster of calcium carbonate biospheroids (bio) from soil fauna activity. Note root channel containing soil fauna excreta to the right. PPL. c) Thin section CGM17 bottom. Clusters of needle fiber calcite from biological activity (arrows). XPL. d) Thin section CGM17 bottom. Bone fragment (bn) with no evidence of combustion. PPL. e) Layer 497D. Thin section CGM17 middle (Fig. 12c). Burnt sediment aggregate (ch). PPL. f) Layer 497D. Thin section CGM17 middle. Anthropogenic sediment aggregate (anthrp). Note light brown/yellowish matrix and embedded charred plant and bone particles of the anthropogenic feature in contrast to geogenic inclusions and reworked textural pedofeature (r) of the reddish non-anthropogenic sediment aggregate (sa). PPL. (For interpretation of the references to colour in this figure legend, the reader is referred to the web version of this article.).

Furthermore development of pedogenic features can be a slow process and reflect long temporal spans associated with the formation dynamics of the stratigraphic record (Farrand, 2001). Therefore, the presence of carbonate pedogenesis in the sediments from facies S1-10 might be indicative also of formation processes involving relatively prolonged intervals of time.

The matrix in facies S1-10 shows similar particle size distribution from the top to the bottom of the accumulation. However, in contrast to S1-30, relative proportions of fines are more heterogeneous in S1-10 (Fig. 4B) reflecting more diverse sediment sources. Fine fraction is composed of 21–26% of sands, and a 74–79% of clayey silts, which show a polymodal distribution, characterised by a secondary peak in the clay fraction (0.29 μm) and the main concentration in the silt fraction, with peaks at 2.5, 5.8, 14.9 and 34.6 μm.

CaO (23%) and organic matter contents (about 22.1%) are considerably lower than those yielded by the samples from facies S1-30 (Table 2). Carbonate values are reflecting in this case a sharp decline in the contribution of anthropogenic debris (i.e. ash) to the sediments.

Organic features in S1-10 are very scarce and characterised by non-combusted plant remains (approximately $\leq 2\% - 500$ μm) and bone fragments ($\leq$4000 μm) (Fig. 14d), which correlates with the lower content of organic matter detected in the compositional results.

Predominance of SiO_2 (33–34%), which doubles the percentages yielded by samples from facies S1-30, can be attributed to the lack of anthropogenic inputs in a matrix where sediment aggregates rich in quartz sand, reddish clay and reworked iron-rich pedofeatures are dominant. Such sedimentary pattern explains also the relatively high values of Al_2O_3 (8.5–8.7%), MgO (4.4–4.8%) and Fe_2O_3 (3.9–4.0%) in samples from S1-10 (Table 2).

Reworked sediments including inputs of *terra rossa* type soils can be found in association with angular rubble in Palaeolithic contexts. Traits of reworked local soils have been detected in caves and rock-shelters holding Middle and Upper Palaeolithic sequences in the Mediterranean area (Farrand, 1979; Goldberg and Bar-Yosef, 1998; Woodward and Goldberg, 2001; Bertrand et al., 2008) as well as in the Iberian Peninsula (Angelucci and Zilhaõ, 2009; Iriarte et al., 2013; Arriolabengoa et al., 2015).

The concentration of reworked sediment aggregates rich in reddish clay and iron-rich pedofeatures in secondary position observed in the thin sections from facies S1-10 suggests, as in S1-20, the accumulation of sediment and soil materials from the immediate context of the site.

According to our data the dynamics involved in the formation of facies S1-10 are closely related to gravity processes in which inputs of translocated sediments rich in soil material as well as rubble from the disaggregation of the rock-shelter roof and walls are dominant.

Intense wetting/drying patterns as showed by the occurrence of large calcitic concretions with marked traits of successive dissolution and recrystallisation dynamics suggest sustained moisture fluctuations during the formation of S1-10. However, in contrast to S1-20, decreasing incidence of redoximorphic features (i.e. *in situ* pedofeatures as opposed to those inherited from reworked soil materials) suggests that the sediments from S1-10 likely underwent shorter periods of water saturation.

Morphoscopic analysis of sand and silt fractions (250–125 μm, 125–63 μm and 63–20 μm) (Fig. 4C) yielded heterogenous results, identifying rounded and also very angular particles. Nevertheless, most of the particles display angular and subangular patterns, which indicates a mainly local source of sediments as in facies S1-30.

Micromorphological results are in agreement with morphoscopy data since only small amounts of rounded particles have been documented in thin section. Concentration and size of these rounded particles in the slides from S1-10 are similar to those observed in samples from S1-20 (Table 1). Furthermore micromorphological analysis indicates that these particles are enclosed in the reworked sediment aggregates rich in reddish soil material, suggesting their inherited nature.

Clay-rich red soils in the Mediterranean region frequently incorporate allochthonous materials as aeolian dust (Fedoroff and Courty, 2013), which supports this hypothesis. Therefore it is possible that the origin of the rounded particles found in the sediments from S1-10 as well as from facies S1-20 is closely related to the translocated soil materials that accumulated in the deposit from above and/or the western lateral of the Ramp sector.

4.3. The sedimentary evidence of the Early UP occupation: layer 497D

A layer of about 6–7 cm thick consisting of subrounded light brown (7.5 YR 6/4) and blackish sediment aggregates and scattered remains of reworked burnt plant and bone tissue is observed at the top of facies S1-10. This accumulation has been documented in an area adjacent to combustion structures which stratigraphic patterns at macroscopic level suggest that they have been preserved *in situ* (Table 1, Figs. 12a and 15a). This layer as well as the adjacent combustion structures present stratigraphic correlation with the artefact accumulation from 497D archaeological level and therefore they can be considered evidence of the Early UP occupation at the site.

Under the microscope the light brown and blackish aggregates show evidence of surface exposure but display distinctive traits that indicate their anthropogenic origin (e.g. unevenly burnt plant and bone tissue). In contrast, sediments from natural origin recorded in the immediate sedimentary context contain features mainly from geogenic and pedogenic sources (Fig. 14e and f).

Micromorphological analysis of one of the combustion structures documented in this sedimentary context (thin section 497D-GC7183) confirms its preservation in primary position (Fig. 15a and b). This combustion structure presents a light brown (7.5 YR 7/4) ashy accumulation at the top and a mixture of dark (7.5 YR 4.1) partially burnt organic and geogenic debris at the bottom (Table 1; Fig. 15c–e). The high proportion of rock fragments and sediment aggregates together with the low concentration of charcoal observed in this dark layer are interpreted as the result of thermal alteration of a palaeosurface, as in the case of the dark layers from facies S1-30.

Burnt patches rich in faecal spherulites and plant remains similar to dung aggregates (e.g., Macphail et al., 1997; Macphail and Goldberg, 2010; Polo-Díaz, 2010) have been documented in this dark layer (Fig. 15f–h). This evidence likely suggests the presence of live fauna at the site predating the combustion episode and therefore the Early UP occupation surface.

The microstratigraphic position of these excremental residues could be considered, as suggested for facies S1-30, an indicator of discontinuity in the occupation of the site by humans. Similar conclusions have been drawn from the occurrence of coprolites in the black layers from the Late MP sequence of El Salt in the Mediterranean rim of the Iberian Peninsula (Mallol et al., 2013b).

As in facies S1-30, micromorphological results from layer 497D are in agreement with outcomes from fabric analysis supporting the sedimentary integrity of the Early UP occupation surface.

Level 497D is detected along the stratigraphic contact between S1-10 and S1-05 (Figs. 3A and 4A). The latter accumulation is interpreted as a breakdown facies from the partial collapse of the roof of the rock-shelter. Facies S1-05, presents scarce matrix and abundant angular limestone boulders that can reach sizes bigger than 1 m. This accumulation of rubble covered up and sealed the archaeological level 497D, separating this layer from the later UP levels included in Unit 497 (i.e. 497A and 497C levels).

Thin sections from sediments overlying S1-10 (CGM17 top and CGM16; Fig. 3B) possibly document facies S1-05 since the location of these samples are next to the area where the concentration of boulders from the roof collapse was documented.

Features in these thin sections present similar characteristics to those observed in S1-10 (Table 1), suggesting continuity in the sedimentary and palaeoenvironmental dynamics at the site.

5. Concluding remarks

5.1. Formation processes of the sterile deposit between the Late MP and the Early UP archaeological layers in Cova Gran have been characterised

Flows rich in local sediment and soil material (facies S1-20) from above and/or the western part of the rock-shelter overlaid and partly altered the top of the MP occupation surface at the westernmost area of the deposit. This entailed partial disturbance of artefact accumulation from S1B and combustion residues from facies S1-30 and S1-25.

Moisture fluctuations were most likely the triggering dynamics favouring mobilisation of materials from the immediate soil and sedimentary context of the site. Partial reworking of the top of the MP sequence explain relative vertical dispersion of the Mousterian assemblage in the area investigated. Subsequent surface stability and a hiatus in the sedimentation favoured soil development under relatively arid to semihumid palaeoenvironmental conditions.

Further sediment accumulation followed (facies S1-10) involving intensification of gravity processes (i.e. inputs from local sediments and soils and clasts from the structure of the rock-shelter) which partly eroded the underlying sediments (facies S1-20). Contrasting wetting/drying cycles documented in the sediments suggest moisture fluctuations as the predominant palaeoenvironmental dynamics at the site during the formation of S1-10. No clear evidence of frost dynamics, sedimentary inputs from long-distance allogenic sources or high-energy dynamics have been

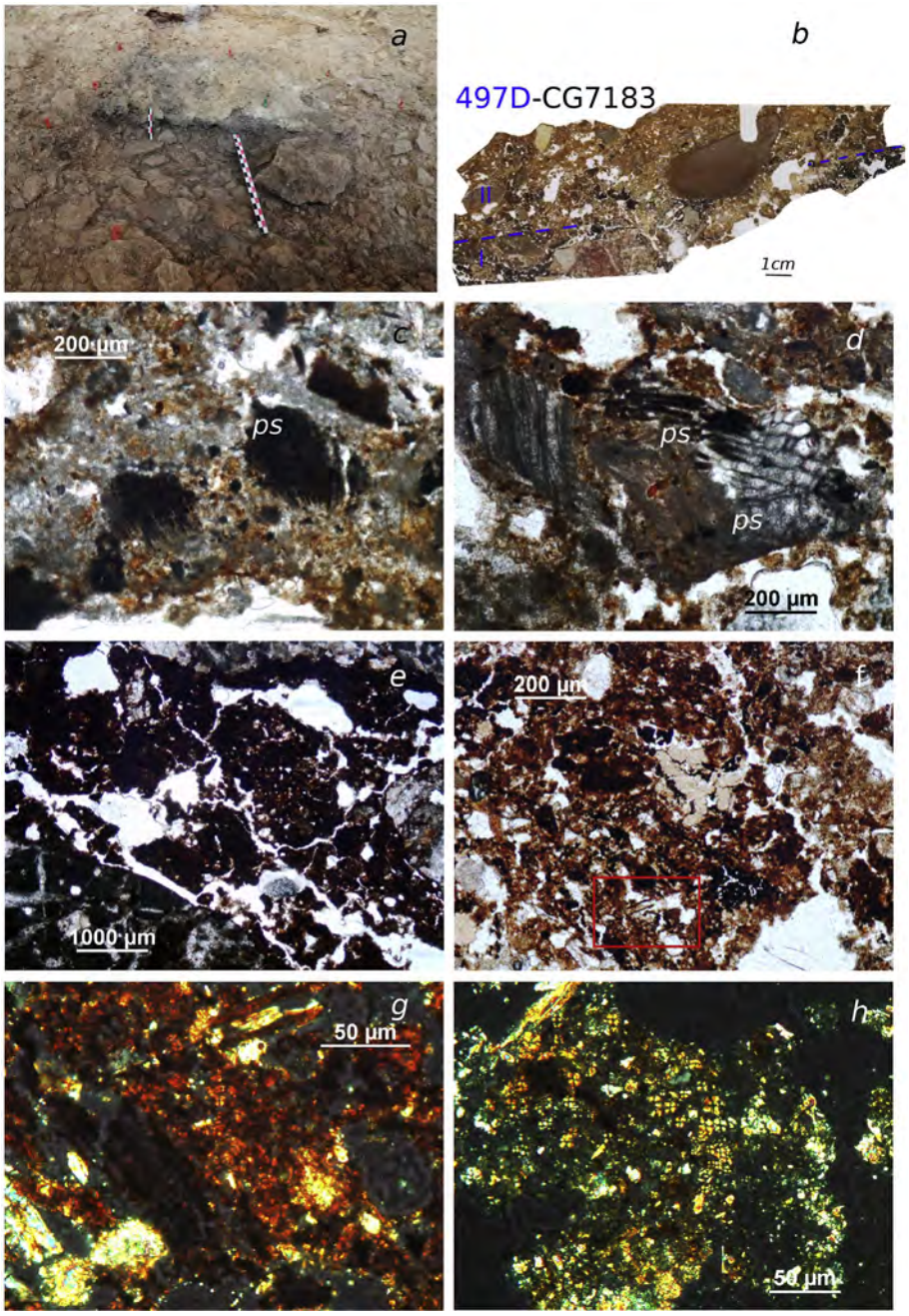

Fig. 15. a) Layer 497D. *In situ* combustion structure during excavation. b) Scan of thin section 497D-CG7183 from the combustion structure pictured in a). Note dark layer containing burnt and charred remains (microfacies I) overlaid by brownish ash accumulation on top (microfacies II). c), d) Thin section 497D-CG7183. Microfacies II. Plant pseudomorphs (ps). PPL. e) Thin section 497D-CG7183. Microfacies I. Charred layer. Note sediment aggregates and rock fragments homogeneously burnt. PPL. f) Thin section 497DCG183. Microfacies I. Charred excrement concentration from the base of the combustion structure. PPL. g) Detail of excrement material pictured in f) (red box). Note plant remains and faecal spherulites embedded in the feature possibly corresponding to herbivore dung. XPL. h) A further example of excremental residue from the same microfacies. Note clusters of faecal spherulites (bright small spheres with a dark cross pattern at the centre). XPL. (For interpretation of the references to colour in this figure legend, the reader is referred to the web version of this article.).

documented. Soil development in S1-10 indicates episodes of surface stability.

Very few traits of anthropogenic features, all of which have been recorded in secondary position, provide support to the hypothesis of sustained discontinuity in the occupation of the site during the formation of S1-10.

Concentration of anthropogenic sediments including *in situ* combustion structures, at the top of the sterile deposit overlying the Mousterian level S1-B, indicates resumed human activity at the site, occurring most likely during an episode of environmental stability. This evidence of human activity correlates with 497D artefact accumulation.

Sediments from facies S1-05 display similar characteristics to those observed in S1-10 suggesting that natural dynamics active at the site during the formation of the sterile deposit had continuity or even intensified after the Early UP occupation of the rock-shelter. Accumulation of rubble from the partial collapse of the roof of the rock-shelter is expression of such dynamics.

5.2. Indicators for the identification of occupation surfaces in contrast to sterile deposits have been provided

From a sedimentary point of view the Late MP occupation surface at Cova Gran is characterised by an extensive ashy accumulation made of overlapping combustion structures (facies S1-30). Hearths are well preserved in their original depositional context.

Characterisation of facies S1-30 as an occupation surface based on sedimentary and stratigraphic parameters allowed its readily distinction from the overlaying sterile deposit, even though sediments from S1-20 and S1-10 enclose anthropogenic features. Indicators of human activity as bone, charcoal and ash are scarce and appear reworked, randomly dispersed and embedded in sediments accumulated by natural dynamics in the sterile deposit.

Sediments from the Early UP occupation surface are characterised by a concentration of reworked anthropogenic residues and *in situ* combustion remains which correlate with 497D artefact accumulation.

Sedimentary and stratigraphic patterns similar to those observed in the occupation surfaces corresponding to facies S1-30 and level 497D have not been detected in the sterile deposit between them.

Full sedimentary and microstratigraphic characterisation of Middle and Upper Palaeolithic occupation surfaces will be provided by investigations currently in progress.

5.3. Microstratigraphic contacts between the sedimentary accumulations of the MUP sequence have been defined

Sediments at the top of the Late MP deposit (facies S1-30) show *in situ* disturbance from dynamics related to surface exposure (i.e. reworking of anthropogenic debris by plant and soil fauna bioturbation and accumulation of rock fragments and biogenic debris including coprolites).

Gradual contact between facies S1-30 and S1-25 together with decreasing concentration of anthropogenic features and intensification of dynamics related to surface exposure indicate a disruption in the accumulation of anthropogenic sediments. This evidence is in agreement with a discontinuity in the occupation of the rock-shelter and the abandonment of the site by humans at the end of the MP.

Sharp contacts detected at the boundary between facies S1-20 and S1-25/S1-30 indicate that at a later point, inputs from the immediate sedimentary and soil context of the rock-shelter entered the site and partially altered the exposed sediments from the top section of the MP sequence.

The accumulation of S1-20 was followed by a period of relative surface stability as indicated by pedogenesis.

Subsequent accumulation of facies S1-10 entailed a further stratigraphic change leaving abrasion marks cutting down into S1-20. The formation of S1-10 is characterised by gravity-related accretion events interspersed by periods of surface stability within a general environmental context of moisture fluctuations. Early UP occupation at the site (layer 497D) took place in this sedimentary and palaeoenvironmental scenario.

5.4. The preservation degree and the integrity of the sequence investigated have been assessed

The formation processes of the MUP sequence at Cova Gran present sedimentary variability in a general palaeoenvironmental context marked by sustained moisture fluctuations.

Both gradual and sharp stratigraphic contacts between occupation surfaces and sterile deposit reflect the syn-post-depositional dynamics involved in the accumulation and alteration of sediments at the MUP boundary.

It has been shown that in a limited area at the top of the MP sequence, incidence of natural dynamics favoured disturbance of the original distribution of Mousterian artefacts. However, results obtained indicate that the overall integrity of the archaeological record was not substantially affected by such processes and that occupation surfaces have been preserved mainly in their original context of deposition.

Our findings also suggest that the rock-shelter was likely abandoned by humans at the end of the MP. In addition no sedimentary evidence of occupation between the MP and the Early UP layers has been documented in the sequence investigated.

Future contributions will address the implications of our results in terms of cultural and settlement patterns at the site during the MUP transition.

This work illustrates the crucial role of geoarchaeology and microstratigraphy for the characterisation and assessment of the interplay between human behaviour and natural dynamics in the formation processes of archaeological records at the MUP boundary.

Acknowledgements

Archaeological investigations at Cova Gran de Santa Linya are funded by the project “Human settlement during the Upper Pleistocene and Holocene in the South-eastern Pyrenees” (HAR2013-42338) of the Spanish Ministry of Economy and Competitiveness as well as by the research group 2014SGR-0084. Fieldwork has been supported by the Serveí d'Arquelogía í Paleontología-Generalítat de Catalunya. Asier Santana Irigoyen manufactured the thin sections. Laser Diffraction and sieving textural analyses were carried out by Leticia Miguéns Rodriguez in the Sample Preparation Laboratory of the CENIEH. WDXRF analytics were conducted by Ana Álvaro Gallo in the Archaeometry Laboratory of the CENIEH. Morphological measures using the Malvern Morphologi G3 were carried out by Silvia González Sierra and Isidoro Campaña Lozano in the Microscopy Laboratory of the same institution. Participants of the WASM held in Basel in 2013 provided valuable micromorphological support. Many thanks to Robyn Inglis and an anonymous reviewer for thoughful comments on the manuscript of this paper.

References

Albert, R.M., Berna, F., Goldberg, P., 2012. Insights on Neanderthal fire use at Kebara Cave (Israel) through high resolution study of prehistoric combustion features: evidence from phytoliths and thin sections. Quaternary International 247, 278–293.

Aleksandrovskii, A.L., 2007. Pyrogenic origin of carbonates: evidence from pedoarchaeological investigation. Eurosian Soil Science 40 (5), 471–477.

Angelucci, D.E., 2010. The recognition and description of knapped lithic artifacts in thin section. Geoarchaeology 25, 220–232.

Angelucci, D.E., Zilhaõ, J., 2009. Stratigraphy and formation processes of the Upper Pleistocene deposit at Gruta da Oliveira, Almonda Karstic System, Torres Novas, Portugal. Geoarchaeology 24, 227–310.

Angelucci, D.E., Anesin, D., Susini, D., Villaverde, V., Zapata, J., Zilhão, J., 2013. Formation processes at a high resolution Middle Paleolithic site: Cueva Antón (Murcia, Spain). Quaternary International 315, 24–41.

Arpin, T., Mallol, C., Goldberg, P., 2002. Short contribution. A new method of analyzing and documenting micromorphological thin sections using flatbed scanners: applications in geoarchaeological studies. Geoarchaeology 17, 305–313.

Arriolabengoa, M., Iriarte, E., Arantza Aranburu, A., Yusta, I., Arrizabalaga, A., 2015. Provenance study of endokarst fine sediments through mineralogical and geochemical data (Lezetxiki II cave, northern Iberia). Quaternary International 364, 231–243.

Aubry, T., Dimuccio, L.A., Almeida, M., Neves, M.J., Angelucci, D.E., Cunha, L., 2011. Palaeoenvironmental forcing during the Middle-Upper Palaeolithic transition in central-western Portugal. Quaternary Research 75, 66–79.
Banks, W.E., d'Errico, F., Zilhão, J., 2013. Human–climate interaction during the Early Upper Paleolithic: testing the hypothesis of an adaptive shift between the Proto-Aurignacian and the Early Aurignacian. Journal of Human Evolution 64, 39–55.
Becze-Deák, J., Langohr, R., Verrecchia, E.P., 1997. Small scale secondary $CaCO_3$ accumulations in selected sections of the european loess belt. Morphological forms and potential for palaenvironmental reconstruction. Geoderma 76, 221–272.
Benito-Calvo, A., Martínez-Moreno, J., Jordá Pardo, J., de la Torre, I., Mora, R., 2009. Sedimentological and archaeological fabrics in Palaeolithic levels of the Southeastern Pyrenees: Cova Gran and Roca dels Bous sites (Lleida, Spain). Journal of Archaeological Sciences 36, 2566–2577.
Benito-Calvo, A., Martínez-Moreno, J., Mora, R., Roy, M., Roda, X., 2011. Trampling experiments at Cova Gran de Santa Linya, Pre-Pyrenees, Spain: their relevance for archaeological fabrics of the Upper-Middle Paleolithic assemblages. Journal of Archaeological Science 38, 3652–3661.
Berna, F., Goldberg, P., 2008. Assessing Paleolithic pyrotechnology and associated hominin behavior in Israel. Israel Journal of Earth Sciences 56, 107–121.
Bernaldo de Quirós, F., Maíllo, J.M., Neira, A., 2008. The place of unit 18 of El Castillo Cave in the middle to upper palaeolithic transition. Eurasian Prehistory 5, 57–72.
Bertran, P., Caner, L., Langohr, R., Lemeé, L., d'Errico, F., 2008. Continental palaeoenvironments during MIS 2 and 3 in southwestern France: the La Ferrassie rockshelter record. Quaternary Science Reviews 27, 2048–2063.
Bertrand, P., Texier, J.-P., 1995. Fabric analysis: application to Palaeolithic sites. Journal of Archaeological Science 22, 521–535.
Bertrand, P., Texier, J.P., 1999. Facies and microfacies of slope deposits. Catena 35, 99–121.
Boixadera, J., Poch, R.M., García-González, M.T., Vizcayno, C., 2003. Hydromorphic and clay-related processes in soils from the Llanos de Moxos (northern Bolivia). Catena 54, 403–424.
Bouma, J., Fox, C.A., Miedema, R., 1990. Micromorphology of hydromorphic soils: applications for soil genesis and land evaluation. In: Douglas, L.A. (Ed.), Soil Micromorphology: a Basic and Applied Science, Developments in Soil Science, vol. 19. Elsevier, Amsterdam, pp. 257–278.
Braadbaart, F., Poole, I., Huisman, H., van Os, B., 2012. Fuel, Fire and Heat: an experimental approach to highlight the potential of studying ash and char remains from archaeological contexts. Journal of Archaeological Science 39, 836–847.
Brochier, J.-E., 1983. Bergeries et feux neolithiques dans le Midi de la France, caracterisation et incidence sur le raisonnement sedimentologique. Quatar Ban 33–34, 181–183.
Brochier, J.-E., 1996. Feullies ou fumiers? Observations sur le role des pussieres spherolitiques dans l'interpretation des depots archeologiques holocenes. Anthropozoologica 24, 19–30.
Brochier, J.-E., 1999. Les Phytolaires. In: Ferdière, A. (Ed.), La Botanique, Collection "Archéologiques". Errance Editions, Paris, pp. 157–170.
Bullock, P., Fédoroff, N., Jongerius, A., Stoops, G., Tursina, T., 1985. Handbook for Soil Thin Section Description. Waine Research Publications, Wolverhampton.
Canti, M.G., 2003. Aspects of the chemical and microscopic characteristics of plant ashes found in archaeological soils. Catena 54, 339–361.
Collcut, S.N., 1979. The analysis of quaternary cave sediments. World Archaeology 10, 290–301.
Costamagno, S., Théry-Parisot, I., Brugal, J.-P., Guibert, R., 2005. Taphonomic consequences of the use of bones as fuel. Experimental data and archaeological applications. In: O'connor, T. (Ed.), Biosphere to Lithopshere. New studies in vertebrate taphonomy. Actes du 9° Colloque de l'ICAZ, Durham, 2002. Oxbow Books, Oxford, pp. 51–62.
Costamagno, S., Théry-Parisot, I., Castel, J.-C., Brugal, J.-P., 2009. Combustible ou non ? Analyse multifactorielle et modèles explicatifs sur des ossements brûlés paléolithiques. In: Théry-Parisot, I., Costamagno, S., Henry, A. (Eds.), Gestion des combustibles au Paléolithique et au Mésolithique: nouveaux outils, nouvelles interprétations, Proceedings of workshop 21. XVeme Congrès de l'UISPP, Lisbonne, 4-9 septembre 2006, BAR International Series 1914. Archaeopress, Oxford, pp. 65–84.
Courty, M.-A., 2001. Microfacies analysis assisting archaeological stratigraphy. In: Goldberg, P., Holliday, V.T., Ferring, C.R. (Eds.), Earth Sciences and Archaeology. Kluwer Academic/Plenum Plublishers, New York, pp. 205–237.
Courty, M.-A., Vallverdù, J., 2001. The microstratigraphic record of abrupt climate change in cave sediments of the Western Mediterranean. Geoarchaeology 5, 467–500.
Courty, M.-A., Carbonell, E., Vallverdú Poch, J., Banerjee, R., 2012. Microstratigraphic and multi-analytical evidence for advanced Neanderthal pyrotechnology at Abric Romani (Capellades, Spain). Quaternary International 247, 294–312.
Courty, M.-A., Goldberg, P., Macphail, R.I., 1989. Soils and Micromorphology in Archaeology. Cambridge University Press.
Durand, N., Monger, H.C., Canti, M., 2010. Calcium carbonate features. In: Stoops, G., Marcelino, V., Mees, F. (Eds.), Interpretation of Micromorphological Features of Soils and Regoliths. Elsevier, Amsterdam, pp. 149–194.
d'Errico, F., Sánchez Goñi, M.F., 2003. Neanderthal extinction and the millennial scale climatic variability of OIS 3. Quaternary Science Reviews 22, 769–788.
Farrand, W.R., 1975. Sediment analysis of a prehistoric rock-shelter: the Abri Pataud. Quaternary Research 5, 1–26.
Farrand, W.R., 1979. Chronology and palaeoenvironment of Levantine prehistoric sites as seen from sediment studies. Journal of Archaeological Science 6, 369–392.
Farrand, W.R., 2001. Sediments and stratigraphy in rockshelters and caves: a personal perspective on principles and pragmatic. In: Woodward, J.C., Goldberg, P. (Eds.), Rock-shelter Sediment Records and Environmental Change in the Mediterranean Region, Geoarchaeology, vol. 16, pp. 537–557. Special Issue.
Fedoroff, N., Courty, M.-A., 2013. Revisiting the genesis of red mediterranean soils. Turkish Journal of Earth Sciences 22, 359–375.
Fedoroff, N., Courty, M.-A., Guo, Z., 2010. Paleosoils and relict soils. In: Stoops, G., Marcelino, V., Mees, F. (Eds.), Interpretation of Micromorphological Features of Soils and Regoliths. Elsevier, Amsterdam, pp. 623–662.
Finlayson, C., Carrión, J.C., 2007. Rapid ecological turnover and its impact on Neanderthal and other human population. Trends in Ecology and Evolution 22, 213–222.
Ford, D., Williams, P., 2007. Karst Hydrogeology and Geomorphology, second ed. Wiley.
Franceschi, V.R., Horner, H.T.J., 1980. Calcium oxalate crystals in plants. The Botanical Review 46, 361–427.
Franceschi, V.R., Nakata, P.A., 2005. Calcium oxalates in plants: formation and funtion. Annual Review of Plant Biology 56, 41–71.
Galván, B., Hernández, C.M., Mallol, C., Mercier, N., Sistiaga, A., Soler, V., 2014. New evidence of early Neanderthal disappearance in the Iberian Peninsula. Journal of Human Evolution 75, 16–27.
Gocke, M., Pustovoytov, K., Kuzyakov, Y., 2012. Pedogenic carbonate formation: recrystallization versus migration—process rates and periods assessed by ^{14}C labeling. Global Biogeochemical Cycles 26, GB1018.
Goldberg, P., Bar-Yosef, O., 1998. Site formation processes in Kebara and Hayonim caves and their significance in Levantine prehistoric caves. In: Akazawa, T., Aoki, K., Bar-Yosef, O. (Eds.), Neandertals and Modern Humans in Western Asia. Plenum, New York, pp. 107–125.
Goldberg, P., Berna, F., 2010. Micromorphology and context. Quaternary International 214, 56–62.
Goldberg, P., Macphail, R.I., 2006. Practical and Theoretical Geoarchaeology. Blackwell Publishing, Oxford.
Goldberg, P., Nathan, Y., 1975. The phosphate mineralogy of et-Tabun cave, Mount Carmel, Israel. Mineralogical Magazine 40, 253–258.
Goldberg, P., Sherwood, S.C., 2006. Deciphering human prehistory through the geoarchaeological study of cave sediments. Evolutionary Anthropology 15, 20–36.
Gómez de la Rúa, D., Mallol, C., Galván, B., Hernández, C.M., 2010. Una visión geoarqueológica general del yacimiento musteriense de El Salt (Alcoy, Alicante) a partir de la micromorfología. Recerques del Museu d'Alcoi 19, 19–32.
Hackett, C.J., 1981. Microscopical focal destruction (tunnels) in exhumed human bones. Medicine Science and Law 21, 243–265.
Iriarte-Avilés, E., Aranburu-Artano, A., Arriolabengoa-Zubizarreta, M., 2013. Geoarqueología de la cueva de Arlanpe (Lemoa, Bizkaia). In: Rios-Garaizar, J., Garate Maidagan, D., Gómez-Olivencia, A. (Eds.), La Cueva de Arlanpe (Lemoa): Ocupaciones Humanas Desde El Paleolítico Medio Antiguo hasta La Prehistoria Reciente, Kobie Serie BAI3. Diputación Foral de Bizkaia, Bilbao, pp. 37–48.
Jackes, M., Sherburne, R., Lubell, D., Barker, C., Wayman, M., 2001. Destruction of microstructure in archaeological bone: a case study from Portugal. International Journal of Osteoarchaeology 11, 415–432.
Jans, M.M., Nielsen-Marsh, C.M., Smith, C.I., Collins, M.J., Kars, H., 2004. Characterization of microbial attack on archaeological bone. Journal of Archaeological Science 31, 87–95.
Karkanas, P., Bar-Yosef, O., Goldberg, P., Weiner, S., 2000. Diagenesis in prehistoric caves: the use of minerals that form in situ to assess the completeness of the archaeological record. Journal of Archaeological Science 27, 915–929.
Karkanas, P., Goldberg, P., 2010. Phosphatic features. In: Stoops, G., Marcelino, V., Mees, F. (Eds.), Interpretation of Micromorphological Features of Soils and Regoliths. Elsevier, Amsterdam, pp. 521–541.
Karkanas, P., Goldberg, P., 2013. Micromorphology of cave sediments. In: Shroder, J., Frumkin, A. (Eds.), Treatise on Geomorphology, Karst Geomorphology, vol. 6. Elsevier, San Diego, pp. 286–297.
Karkanas, P., Kyparissi-Apostolika, N., Bar-Yosef, O., Weiner, S., 1999. Mineral assemblages in Theopetra, Greece: a framework for understanding diagenesis in a prehistoric cave. Journal of Archaeological Science 26, 1171–1180.
Karkanas, P., Rigaud, J.-P., Simek, J.F., Albert, R.M., Weiner, S., 2002. Ash bones and guano: a study of the minerals and phytoliths in the sediments of Grotte XVI, Dordogne, France. Journal of Archaeological Science 29, 721–732.
Kehl, M., Eckmeier, E., Franz, S.O., Lehmkuhl, F., Soler, J., Soler, N., Reicherter, K., Weniger, G.C., 2014. Sediment sequence and site formation processes at the Arbreda Cave, NE Iberian Peninsula, and implications on human occupation and climate change during the Last Glacial. Climate of the Past 10, 1673–1692.
Khokhlova, O.S., Sedov, S.N., Golyeva, A.A., Khokhlov, A.A., 2001. Evolution of Chenozems in the Northern Caucasus, Russia during the second half of the Holocene: carbonate status of Paleosols as a tool for paleoenvironmental reconstruction. Geoderma 4, 115–133.
Khormali, F., Abtahi, A., Stoops, G., 2006. Micromorphology of calcitic features in highly calcareous soils of fars province, Southern Iran. Geoderma 132, 31–46.
Laville, H., 1976. Deposits in calcareous rock shelters: analytical methods and climatic interpretation. In: Davidson, D.A., Shackley, M.I. (Eds.), Geoarchaeology. Duckworth, London, pp. 137–155.
Laville, H., Rigaud, J.-P., Sackett, J., 1980. The Rock-Shelters of the Perigord. Academic Press, New York.

Lenoble, A., Bertrand, P., 2004. Fabric of paleolithic levels: methods and implications for site formation processes. Journal of Archaeological Science 31, 457–469.
Lenoble, A., Bertran, P., Lacrampe, F., 2008. Solifluction-induced modifications of archaeological levels: simulation based on experimental data from a modern periglacial slope and application of French Palaeolithic sites. Journal of Archaeological Science 35, 99–110.
Lindbo, D.L., Stolt, M.H., Vepraskas, M.J., 2010. Redoximorphic features. In: Stoops, G., Marcelino, V., Mees, F. (Eds.), Interpretation of Micromorphological Features of Soils and Regoliths. Elsevier, Amsterdam, pp. 129–147.
Macphail, R.I., Courty, M.-A., Hather, J., Wattez, J., 1997. The soil micromorphological evidence of domestic occupation and stabling activities. In: Maggi, R. (Ed.), Arene Candide: a Functional and Environmental Assessment of the Holocene Sequences Excavated by L. Bernabo' Brea (1940-1950), Memorie dell'Istituto Italiano di Paleontologia Umana, V. Istituto Italiano de Paleontologia Umana, Roma, pp. 53–88.
Macphail, R.I., Goldberg, P., 2010. Archaeological materials. In: Stoops, G., Marcelino, V., Mees, F. (Eds.), Interpretation of Micromorphological Features of Soils and Regoliths. Elsevier, Amsterdam, pp. 589–622.
Mallol, C., Cabanes, D., Baena, J., 2010. Microstratigraphy and diagenesis at the upper Pleistocene site of Esquilleu Cave (Cantabria, Spain). Quaternary International 214, 70–81.
Mallol, C., Hernández, C.M., Cabanes, D., Machado, J., Sistiaga, A., Pérez, P., Galván, B., 2013a. Human actions performed on simple combustion structures: an experimental approach to the study of Middle Palaeolithic fire. Quaternary International 315, 3–15.
Mallol, C., Hernández, C., Machado, J., 2012. The significance of stratigraphic discontinuities in Iberian Middle-to-Upper Palaeolithic transitional sites. Quaternary International 275, 4–13.
Mallol, C., Hernández, C.M., Cabanes, D., Sistiaga, A., Machado, J., Rodríguez, A., Perez, L., Galvan, B., 2013b. The black layer of Middle Palaeolithic combustion structures. Interpretations and archaeostratigraphic implications. Journal of Archaeological Science 40, 2515–2537.
Manafi, S., Poch, R.M., 2012. Micromorphic pedofeatures related to pedogenic calcium carbonate in some arid and semiarid soils in the west of Urmia Lake, Iran. In: Proceedings of the 14th International Working Meeting on Soil Micromorphology. Lleida 8–14 July 2012.
Martínez-Moreno, J., Mora, R., de la Torre, I., 2010. The Middle-to-Upper Palaeolithic transition in Cova Gran and the extinction of Neanderthals in the Iberian Peninsula. Journal of Human Evolution 58, 211–226.
McPherron, S.J.P., 2005. Artifact orientation and site formation processes from total station proveniences. Journal of Archaeological Science 32, 1003–1014.
Mentzer, S., 2014. Microarchaeological approaches to the identification and interpretation of combustion features in archaeological sites. Journal of Archaeological Method and Theory 21, 616–668.
Miller, C.E., Conard, N.J., Goldberg, P., Berna, F., 2010. Dumping, sweeping and trampling: experimental micromorphological analysis of anthropogenically modified combustion features. Palethnologie 2, 25–37.
Mora, R., Benito-Calvo, A., Martínez-Moreno, J., González Marcen, P., de la Torre, I., 2011. Chrono-stratigraphy of the Upper Pleistocene and Holocene archaeological sequence in Cova Gran (south-eastern Pre-Pyrenees, Iberian Peninsula). Journal of Quaternary Science 26, 635–644.
Mora-Torcal, R., Benito-Calvo, A., Martínez-Moreno, J., de la Torre, I., Vega Bolivar, S., Roy, M., Roda Gilabert, X., Samper Carro, S., 2014. A key sequence in the Western Mediterranean prehistory: Cova Gran de Santa Linya (Pre-Pyrenees in Lleida). In: Ramos, Sala (Ed.), Pleistocene and Holocene Hunter–gatherers in Iberia and the Gibraltar Strait: the Current Archaeological Record. Universidad de Burgos and Fundación Atapuerca, Burgos, pp. 162–166.
Mora-Torcal, R., Martínez-Moreno, J., Roy-Sunyer, M., Benito-Calvo, A., Polo-Díaz, A. Samper-Carro, S., (under review). Contextual, techno-typological and chronometric implications from Cova Gran to the Middle-to-Upper Palaeolithic debate in Northeastern Iberia.
Nicholson, R.A., 1993. A morphological investigation of burnt animal bone and an evaluation of its utility in archaeology. Journal of Archaeological Science 20, 411–428.
Ninyerola, M., Pons, X., Roure, J.M., 2005. Atlas Climático Digital de la Península Ibérica. Metodología y aplicaciones en bioclimatología y geobotánica. Universidad Autónoma de Barcelona, Bellaterra. ISBN 932860-8-7.
Ould, M., Bruand, A., 1994. Morphology and origin of secondary calcite in soils from Beauce, France. In: Ringrose-Voase, A.J., Humphreys, G.S. (Eds.), Soil Management and Genesis. Elsevier, Amsterdam, pp. 27–36.
Piperno, D.R., 1988. Phytoliths Analysis, an Achaeological and Geological Perspective. Academic Press, San Diego.
Polo-Díaz, A., 2010. Rediles prehistóricos y uso del espacio en abrigos bajo roca en la Cuenca Alta del Ebro: geoarqueología y procesos de formación durante el Holoceno. Unpublished Ph.D. thesis. Universidad del País Vasco-Euskal Herriko Unibertsitatea (UPV-EHU).
Polo-Díaz, A., Fernández Eraso, J., 2010. Same anthropogenic activity, different taphonomic processes: a comparison of sediments from two neighboring prehistoric rockshelter deposits (Los Husos I and Los Husos II, Upper Ebro Basin, Spain). Quaternary International 214, 82–97.
Roy Sunyer, M., Roda Gilabert, X., Benito-Calvo, A., Martínez-Moreno, J., Mora Torcal, R., 2014. Verificando la integridad del registro arqueológico: análisis de fábricas en las unidades arqueológicas del paleolítico medio/superior de la Cova Gran (Santa Linya, Lleida). Treballs d'Arqueologia 20, 55–77.
Schiegl, S., Goldberg, P., Bar Yosef, O., Weiner, S., 1996. Ash deposits in Hayonim and Kebara Caves, Israel: macroscopic, microscopic and mineralogical observations, and their archaeological implications. Journal of Archaeological Science 23, 763–781.
Schiegl, S., Goldberg, P., Pfretzschner, H.-U., Conard, N.J., 2003. Paleolithic burnt bone horizons from the Swabian Jura: distinguishing between *in situ* fireplaces and dumping areas. Geoarchaeology 18, 541–565.
Schmidt, I., Bradtmöller, M., Kehl, M., Pastoors, A., Tafelmaier, Y., Weninger, B., Weniger, G.-C., 2012. Rapid climate change and variability of settlement patterns in Iberia during the Late Pleistocene: temporal and spatial corridors of Homo sapiens sapiens population dynamics during the Late Pleistocene and Early Holocene. Quaternary International 274, 179–204.
Sepulchre, P., Ramstein, G., Kageyama, M., Vanhaeren, M., Krinner, G., Sánchez-Goñi, M.-F., d'Errico, F., 2007. H4 abrupt even and late Neanderthal presence in Iberia. Earth and Planetary Science Letters 258, 283–292.
Servei Meteorològic de Catalunya, 2014. Meteocat (Online). http://www.meteo.cat/.
Shahack-Gross, R., Berna, F., Karkanas, P., Weiner, S., 2004. Bat guano and preservation of archaeological remains in cave sites. Journal of Archaeological Science 31, 1259–1272.
Simó, A., 2004. La Cordillera Pirenaica. 3.5.9: El Cretácico superior de la Unidad Surpirenaica central. In: Avera, J.A. (Ed.), Geología de España. Sociedad geológica de España/Instituto geológico y minero de España, Madrid, pp. 296–299.
Soler i Subils, J., Soler i Masferrer, N., Maroto, J., 2008. L'Arbreda Archaic Aurignacian dates clarified. Eurasian Prehistory 5, 45–56.
Stiner, M.C., Kuhn, S.L., Weiner, S., Bar Yoserf, O., 1995. Differential burning, recrystallization and fragmentation of archaeological bone. Journal of Archaeological Science 22, 223–237.
Stoops, G., 2003. Guidelines for Analysis and Description of Soil and Regolith Thin Sections. Soil Science Society of America, Madison.
Théry-Parisot, I., Costamagno, S., 2005. Propriétés combustibles des ossements: données expérimentales et réflexions archéologiques sur leur emploi dans les sites paléolithiques. Gallia préhistoire 47, 235–254.
Vallverdú, J., Vaquero, M., Cáceres, I., Allué, E., Rosell, J., Saladié, P., Chacón, G., Ollé, A., Canals, A., Sala, R., Courty, M.-A., Carbonell, E., 2010. Sleeping activity area within the site structure of Archaic human groups: evidence from Abric Romaní level N combustion activity areas. Current Anthropology 51, 137–145.
Verrecchia, E., 2002. Géodynamique du carbonate de calcium à la surface des continents. In: Miskovsky, J.C. (Ed.), Géologie de la préhistoire. Geopré, Paris, pp. 233–258.
Verrecchia, E.P., Verrecchia, K.E., 1994. Needle-fiber calcite: a critical review and a proposed classification. Journal of Sedimentary Research A64, 650–664.
Vidal-Matutano, P., Hernández, C.M., Galván, B., Mallol, C., 2015. Neanderthal firewood management: evidence from Stratigraphic Unit IV of Abric del Pastor (Eastern Iberia). Quaternary Science Reviews 111, 81–93.
Van Vliet-Lanoë, B., 1987. Dynamique périglaciaire actuelle et passée. Apport de l'étude micromorphologique et de l'expérimentation. Bulletin de l'Association Française pour l'Etude du Quaternarie 2, 113–132.
Van Vliet-Lanoë, B., 1998. Frost and soils: implications for paleosols, paleoclimates and stratigraphy. Catena 34, 157–183.
Wattez, J., 1992. Dynamique de formation des structures de combustion de la fin du Paleolithique au Neolithique moyen: approche methodologique et implications culturelles. These de Nouveau Doctorat. Université de Paris.
Wattez, J., Courty, M.-A., 1987. Morphology of ash of some plant materials. In: Fedoroff, N., Bresson, I-M., Courty, M.-A. (Eds.). Soil micromorphology. Éditions de l'Association Française pour l'Etude des Sols, Paris, pp. 677–683.
Wattez, J., Courty, M.-A., Macphail, R.I., 1990. Burnt organo-mineral deposits related to animal and human activities in prehistoric caves. In: Douglas, L.A. (Ed.), Soil Micromorphology. Elsevier, Amsterdam, pp. 431–439.
Weiner, S., Goldberg, P., Bar Yoserf, O., 1993. Bone preservation in Kebara cave, Israel using on-site fourier transform infrared spectrometry. Journal of Archaeological Science 20, 613–627.
Weiner, S., Goldberg, P., Bar-Yosef, O., 2002. Three-dimensional distribution of minerals in the sediments of Hayonim cave, Israel: diagenetic processes and archaeological implications. Journal of Archaeological Science 29, 1289–1308.
Woodward, J.C., Bailey, G.N., 2000. Sediment sources and terminal Pleistocene geomorphological processes recorded in rock-shelter sequences in Northwest Greece. In: Foster, I.D.L. (Ed.), Tracers in Geomorphology. Wiley, Chichester, pp. 521–551.
Woodward, J.C., Goldberg, P., 2001. The sedimentary records in Mediterranean rockshelters and caves: archives of environmental change. Geoarchaeology 16, 327–354.
Zilhão, J., 2006a. Neanderthals and moderns mixed, and it matters. Evolutionary Anthropology 15, 183–195.
Zilhão, J., 2006b. Chronostratigraphy of the Middle-to-Upper Paleolithic transition in the Iberian Peninsula. Pyrenae 37, 7–84.
Zilhão, J., d'Errico, F., 1999. The chronology and taphonomy of the earliest Aurignacian and its implications for the understanding of Neandertal extinction. Journal of World Prehistory 13, 1–68.